Causal-Discovery Signals Between Climatic and Socioeconomic Candidate Correlates and Antimicrobial Resistance in Escherichia coli

Özlem Baydaroğlu

Graduate School of Informatics, Middle East Technical University, Ankara, Türkiye

National Academies of Sciences, Engineering, and Medicine, Washington, DC, US

Abstract

Antimicrobial resistance (AMR) is a rapidly escalating global health crisis threatening human, animal, and environmental well-being. While its spread is often linked to antibiotic use, its environmental and socioeconomic drivers remain poorly understood. This study investigates observational causal-discovery signals between AMR and climatic and socioeconomic drivers across 49 U.S. states, using annual state-level data from 2011 to 2024. Resistance data for four *Escherichia coli* phenotypes (carbapenem-, multidrug-, cephalosporin-, and fluoroquinolone-resistant) have been pooled as independent annual realizations, increasing the effective sample size given the limited (14-year) depth of state-level surveillance. Three complementary methods (PCMCI, CCM, and TE) have been applied in parallel, with false-discovery-rate correction and cross-method consensus used to assess robustness. Results reveal a heterogeneous landscape of directional associations, with maximum and minimum temperature, precipitation, and per capita income associated with AMR in a subset of states. After Benjamini–Hochberg correction, no state–driver association has remained significant in more than one method (FDR $p < 0.05$: PCMCI, 7 pairs; CCM, 1; TE, 0). The single association identified by all three methods at the nominal level (maximum temperature in West Virginia) therefore represents a candidate signal for follow-up rather than a confirmed finding, reflecting the limited statistical power of short annual series. These findings nonetheless suggest that climatic and socioeconomic conditions merit consideration alongside antimicrobial-use factors, supporting phenotype-specific, regionally informed AMR surveillance within a One Health framework.

Keywords: Antimicrobial Resistance (AMR), Climate Variability, Escherichia coli, Causal Discovery, One Health

---

This manuscript is an EarthArXiv preprint and has been submitted for possible publication in a peer-reviewed journal. Please note that this has not been peer-reviewed before and is currently undergoing peer review for the first time. Subsequent versions of this manuscript may have slightly different content.

---

1. Introduction

Antimicrobial resistance (AMR) refers to the capacity of microorganisms, including bacteria, viruses, or parasites, to withstand the effects of antibiotics, hence rendering them ineffective. The health of people, animals, and ecosystems can be severely impacted by bacteria that become persistent and spread when antibiotics employed in treatments prove unsuccessful and infections endure.

The World Health Organization reports that bacterial AMR was directly responsible for 1.27 million deaths and associated with a further 4.95 million deaths worldwide in 2019 (Murray et al., 2022). More recent global burden estimates place the annual toll at 1.14 million attributable deaths in 2021, projected to rise to 1.91 million annually by 2050 (Naghavi et al., 2024).

According to the 2019 Antibiotic Resistance Threats Report by the Centers for Disease Control and Prevention (CDC), over 2.8 million AMR infections occur annually in the US, resulting in more than 35,000 deaths (CDC, 2019). Furthermore, the CDC indicates that AMR incurs an additional $20 billion in direct healthcare expenses in the US, excluding around $35 billion in annual productivity losses (Dadgostar, 2019). In consideration of the facts, during the 79th United Nations General Assembly (UNGA) HLM on AMR in 2024, global leaders pledged to decrease human fatalities from AMR by 10% by 2030 (United Nations General Assembly, 2024). In summary, AMR poses a significant threat to global health, necessitating study and mitigation initiatives. Despite the current surge in AMR research, scant investigation has been undertaken, especially in low- and middle-income nations, regarding the dynamic interplay of AMR with climate change and socioeconomic factors (Kirby and Herbert, 2013; Booth and Wester, 2022; Li et al., 2025; Moon et al., 2025).

Although there are studies investigating the correlation between AMR and meteorological, environmental, social, and political factors, research focusing on causative links is notably scarce. Zhao et al. (2024) used bioinformatics and AI to predict antibiotic resistance gene traits. Causal-ARG, a CNN framework with Gaussian Mixture Model (GMM), stresses gene causality, encompassing mechanism, phenotype, and antibiotic class. Using a dataset from 70 middle- and high-income countries, Awasthi et al. (2022) analyzed AMR determinants using Bayesian Network and counterfactual analysis. Structural changes in countries with poor healthcare systems may lower resistance by 50%, according to their research. Donaghy et al. (2019) examined how cleaning and disinfectants affect AMR. The study compared laboratory trials with food processing facility field studies using literature synthesis and scientific review. The authors noted that while bacteria can evolve resistance to low doses of disinfectants in a lab, there is no compelling evidence that disinfectants used at correct quantities contribute to the global AMR crisis. Martínez et al. (2025) studied the dynamic interaction and temporal lag effects of AMR in primary care and hospitals. Their approach included multivariable logistic regressions, vector autoregressive models, and Granger (Granger, 1969) causality analyses. Resistance

rates in primary care and hospitals were positively correlated, showing that as community resistance rises, so does hospital resistance. Hospital *E. coli* (Escherichia coli) resistance was predicted by community resistance changes. To visualize how AMR works, Huebner et al. (2025) used a Causal Loop Diagram to map the reinforcing and balancing relationships between various elements. This study used questionnaires, semi-structured interviews, and interactive workshops to obtain data. Environmental factors like wastewater treatment plant-derived resistance genes and bacteria fertilizing soil and groundwater were evaluated. Since each region has unique agricultural, health, and environmental characteristics, the authors conclude that the global AMR crisis must be tackled regionally.

Some of the methods employed in causality studies include Granger causality; transfer entropy (TE) (Schreiber, 2000), which is grounded in information theory (Shannon, 1948; Baydaroğlu and Koçak, 2019); convergent cross mapping (CCM) (Sugihara et al., 2012), based on Takens' theorem (Takens, 2006; Baydaroğlu et al., 2024; Baydaroğlu, 2025); and the stochastic framework for testing conditional independence known as PCMCI (Peter and Clark Momentary Conditional Independence), originally introduced by Runge et al. (2019b) and subsequently applied across environmental and hydroclimatic contexts (Delforge, 2022; Yeşilköy et al., 2026). PCMCI is a two-stage procedure based on the PC (Peter–Clark) algorithm (Spirtes and Glymour, 1991), followed by a momentary conditional independence (MCI) test that controls for autocorrelation and indirect effects (Runge et al., 2015, 2019b).

Adopting a One Health approach, this study investigates causal-discovery signals between AMR in *E. coli* and key climatic drivers (maximum temperature, minimum temperature, and precipitation) and socioeconomic factors (per capita personal income, PCPI), using annual state-level data spanning 2011–2024 across the United States. Resistance data from four *E. coli* phenotypes—carbapenem-resistant, multidrug (MDR)-resistant, cephalosporin-resistant, and fluoroquinolone-resistant strains—have been pooled as independent realizations of the same underlying process to increase the effective sample size available for causal discovery. Three complementary causal-discovery and information-theoretic methods, PCMCI, CCM, and TE, have been applied in parallel to identify directional associations, with multiple testing correction and cross-method agreement used to assess the robustness of findings. This multidisciplinary, data-driven approach aims to inform regionally tailored strategies for addressing this critical threat to human, animal, and ecosystem health.

2. Background

AMR is a global concern impacting the health of both humans and animals. Although AMR predominantly arises from the excessive and improper use of antibiotics and antimicrobials, compelling evidence indicates that the broader dissemination of resistance is exacerbated by additional factors, including insufficient local sanitation (Ljungqvist et al., 2025), environmental contamination, agricultural applications (Csorba

et al., 2025), and climate change, with the natural environment serving as a crucial vector in this phenomenon (Woolhouse et al., 2015; Graham et al., 2019; Al-Khalaifah et al., 2025).

A growing body of large-scale observational work supports this view. Li et al. (2025), drawing on 4502 AMR surveillance records from 101 countries, linked environmental and social variables to AMR trajectories under diverse socioeconomic pathways, finding a widening gap between high- and low/middle-income nations. Zambrano (2023) argued that environmental contaminants, extreme weather, and land-use change accelerate the anthropogenic spread of resistance genes through shared wildlife–human reservoirs and waterway "highways."

Kalanxhi and Laxminarayan (2026) proposed three specific mechanisms linking climate to AMR: temperature-driven increases in bacterial proliferation and horizontal gene transfer; disaster-driven increases in infection burden and antibiotic use; and rainfall-driven dissemination of resistance genes through wastewater and runoff. At the genomic scale, Wang et al. (2025), analyzing 208233 Salmonella genomes from 148 countries, identified socioeconomic indicators (GDP, healthcare expenditure, and education); climate; pollution; and global trade and travel as critical determinants of resistance trends. Consistent with these findings, a broader literature has linked ambient and air temperature (Zeng et al., 2023; MacFadden et al., 2018; Rodríguez-Verdugo et al., 2020; Meinen et al., 2023; Ching et al., 2025; Yang et al., 2026; Kou et al., 2025; Kalanxhi and Laxminarayan, 2026), precipitation and extreme weather (Ching et al., 2025; Usman Qamar and Aatika, 2023; Csorba et al., 2025), and agricultural, water, soil, and air pollution pathways (Gao et al., 2024; Booth and Wester, 2022; Zhou et al., 2024; Díaz-Zaragoza et al., 2025; Chayña et al., 2025; Yazdankhah et al., 2018; Kou et al., 2025; Özbek, 2026; Matijašević, 2026) to the emergence and proliferation of AMR. Collectively, these studies establish correlational or mechanistic associations between climatic, environmental, and socioeconomic factors and AMR at global and regional scales, but few apply formal causal-discovery frameworks capable of distinguishing directional, temporally resolved dependence from simple co-occurrence or confounding.

E. coli is a leading cause of both community- and hospital-acquired infections, particularly urinary tract and bloodstream infections, and resistant strains are associated with more severe outcomes, reduced effectiveness of empirical treatment, and substantial healthcare costs (MacKinnon et al., 2020). Untreated or insufficiently treated drinking water is a major source of resistant *E. coli*; resistant strains further propagate through the food chain via antibiotic-exposed livestock, agricultural runoff, and incomplete removal by wastewater treatment, with precipitation acting as an additional transport pathway for urban and agricultural contaminants into water bodies (Booth and Wester, 2022).

Prior work on *E. coli* specifically has examined complementary but narrower angles of this problem. Rodríguez-Verdugo et al. (2020) showed experimentally that higher growth temperatures accelerate the emergence of antibiotic-resistance mutations.

Leekitcharoenphon et al. (2021) documented widespread and variable AMR gene dissemination across European livestock, identifying poultry as a particularly informative indicator group. Kou et al. (2025) applied a spatial Durbin model to a decade of Chinese surveillance data and found that resistance clusters spatially, with ambient temperature and $PM_{2.5}$ pollution both contributing to elevated resistance in neighboring provinces. At the governance level, Collignon et al. (2015) found that corruption and weak regulatory enforcement predict cross-national AMR patterns more strongly than antibiotic consumption itself. Together, these studies point to temperature, spatial clustering, and governance as important correlates of *E. coli* resistance, yet none apply a multi-method causal-discovery framework capable of jointly evaluating climatic and socioeconomic drivers across multiple resistance phenotypes at sub-national (state) resolution. This gap motivates the present study's use of PCMCI, CCM, and TE to assess directional associations between climatic and socioeconomic conditions and *E. coli* resistance across U.S. states, using resistance data pooled across four phenotypes to compensate for the limited temporal depth of state-level AMR surveillance.

3. Materials and Methods

3.1 Study Area

The study covers 49 U.S. states, excluding Washington, D.C. and Wyoming, both of which lacked CDC AMR surveillance records across the study period. Resistance data for all four phenotypes have been pooled for 46 states; for the remaining three states (Alaska, Delaware, and North Dakota), carbapenem-resistant *E. coli* data availability fell below that of other states and has been excluded from pooling for that state, yielding a correspondingly smaller number of pooled phenotype-year observations (n = 39, 42, and 31, respectively). Among the 46 states with complete four-phenotype pooling, the number of pooled phenotype-year observations ranged from 51 to 56; values below the theoretical maximum of 56 (14 years × 4 phenotypes) reflect the unavailability of 2011 data for a subset of states in the CDC AMR surveillance program's inaugural year, and, for Vermont, an additional missing year (2013) in the cephalosporin-resistant phenotype. Full state-level details are provided in Table S1.

3.2 Data

This study utilizes state-level data spanning from 2011 to 2024, focusing on the dynamics of AMR in *E. coli*, a key coliform bacterium. The dataset, provided by the CDC, comprises state-level annual observations of the "percent resistant" metric for four *E. coli* resistance phenotypes—carbapenem-resistant, multidrug (MDR)-resistant, cephalosporin-resistant, and fluoroquinolone-resistant strains—which have been pooled as independent annual realizations for each state in the causal-discovery analyses. "Percent resistant" has been extracted for the CDC's "All Infectious Event Type Data" category, in which resistance percentages are calculated across all reported clinical specimens and infection sources combined, rather than restricted to a specific infection site or specimen type. Consistent with CDC reporting conventions, percent-resistant values are not published by the CDC

when the underlying number of tested isolates for a given state-year-phenotype combination falls below a minimum reliability threshold (n < 20); such state-years are therefore absent from the source data rather than actively excluded.

The meteorological parameters utilized in this study consist of monthly maximum and minimum temperatures ($°F$; $°C = (°F - 32) \times 5/9$) and total monthly precipitation (inches; $1\ inch = 25.4\ mm$), all sourced from the NOAA National Centers for Environmental Information (NCEI). These monthly values were aggregated to the annual scale for each state-year as follows: Annual maximum temperature (Tmax) was defined as the highest of the twelve monthly maximum values; annual minimum temperature (Tmin) was defined as the lowest of the twelve monthly minimum values; and annual precipitation was defined as the sum of the twelve monthly total precipitation values. To account for socioeconomic factors, annual per capita personal income (PCPI) data were obtained directly at annual resolution from the U.S. Bureau of Economic Analysis (BEA).

All datasets have been integrated to investigate the drivers of AMR within a One Health framework. Before turning to the causal-discovery analyses, This section first present a descriptive overview of *E. coli* AMR trends across the study period. Figure 1 shows the mean annual AMR rate across all four resistance phenotypes and all included states, illustrating a general upward trend in resistance levels over 2011–2024, punctuated by notable declines in 2012 and 2021 and a period of relative stagnation between 2017 and 2019. Because Figure 1 pools four phenotypes with different baseline prevalence and resistance characteristics into a single mean trend, it is intended as a descriptive overview of aggregate temporal patterns rather than as a basis for inference; the proposed explanations for the 2012 and 2021 inflections below are offered as hypotheses motivating future investigation. Figure 2 (a–d) presents the corresponding annual AMR trends separately for each of the four resistance phenotypes.

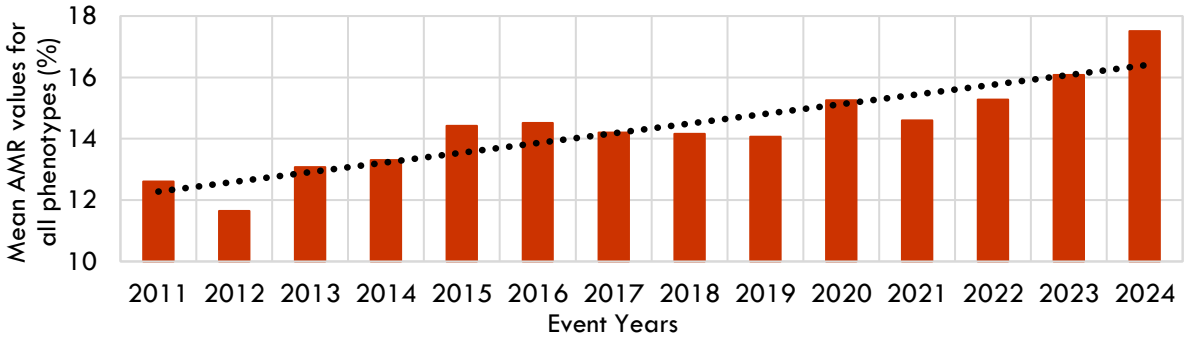
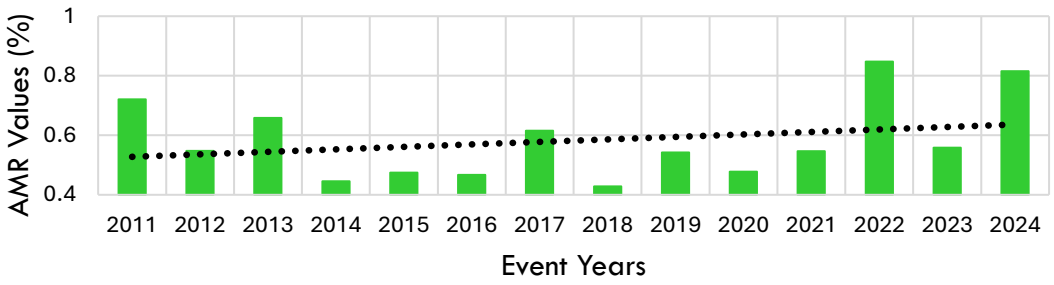


Figure 1. Mean AMR values for all phenotypes based on event years.

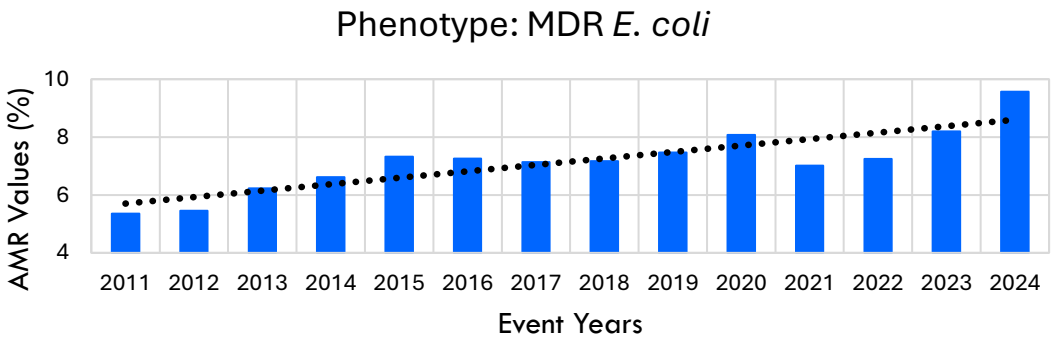
In Figure 1, the results show notable declines in *E. coli* AMR levels in 2012 and 2021. The decline observed in 2012 coincides with the introduction of the FDA's Guidance for Industry #209, which established a voluntary framework to limit the subtherapeutic use of medically important antibiotics in livestock (FDA, 2012; Alvy, 2014; Deb et al., 2023); a

plausible but untested hypothesis is that this policy shift contributed to the observed decline. Similarly, the 2021 decrease may plausibly reflect secondary effects of the COVID-19 pandemic, during which unprecedented changes in hygiene practices, social distancing, and healthcare utilization have been suggested to temporarily disrupt transmission cycles of resistant bacteria (CDC, 2022).

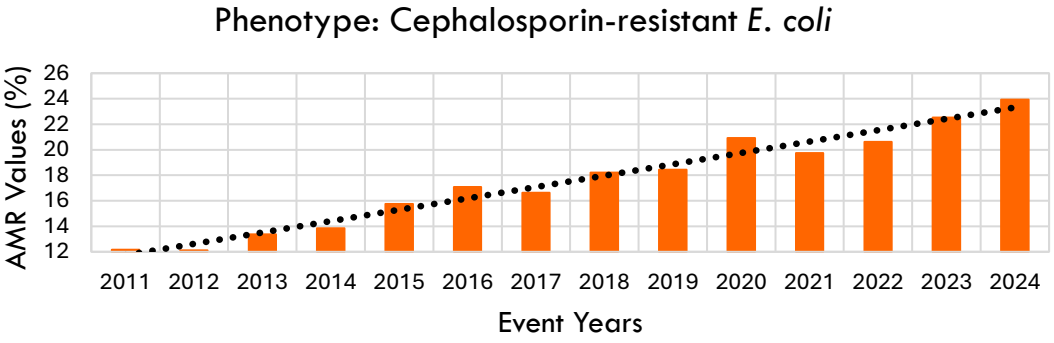
(a)



(b)



(c)



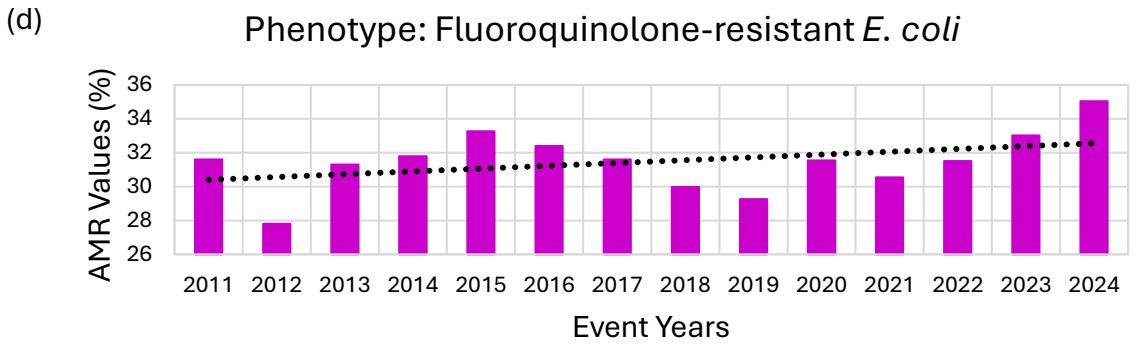


Figure 2. Between the years 2011 and 2024, AMR values for (a) Phenotype: Carbapenem-resistant *E. coli* (b) Phenotype: MDR *E. coli* (c) Phenotype: Cephalosporin-resistant *E. coli* (d) Phenotype: Fluoroquinolone-resistant *E. coli*.

The analysis of the alterations in resistance phenotypes of *E. coli* to four distinct antibiotic classes over time reveals a rise in AMR rates for each phenotype (see Figure 2 (a-d)). Figure 2 (a-d) indicates that the AMR rates of *E. coli* across all phenotypes demonstrate an increasing trend over the years. The rise is more significant for MDR-resistant and cephalosporin-resistant *E. coli*, but the AMR values for carbapenem-resistant and fluoroquinolone-resistant *E. coli* exhibit fluctuation. The resistance percentages of MDR-resistant and cephalosporin-resistant *E. coli* exhibit a steadily increasing trend.

As highlighted by Bartsev et al. (2021) and Bonotto et al. (2022), the presence of underlying trends and seasonality in time-series data can lead to spurious causality. To mitigate this risk, both the AMR series and each candidate driver (temperature, precipitation, and PCPI) have been linearly detrended prior to analysis. Given that the dataset consists of annual observations, seasonality has not been considered a factor influencing the time-series characteristics.

3.3 Methods

This study employs a unified causal-discovery framework to examine the relationship between AMR in *E. coli* and candidate climatic and socioeconomic drivers, comprising climatic factors (precipitation, maximum temperature, and minimum temperature) and a socioeconomic indicator (per capita personal income, PCPI). Rather than analyzing each of the four resistance phenotypes independently—an approach constrained by the limited length (14 years) of state-level annual AMR records—resistance data for the four phenotypes have been pooled as independent annual realizations of the same underlying process for each state, increasing the effective sample size available for causal discovery.

Three complementary methods have been applied: PCMCI, TE, and CCM. Both the AMR series and each candidate driver have been linearly detrended prior to analysis for all three methods. Pooling across phenotypes has been implemented in a manner appropriate to each method: for PCMCI, the four phenotypes have been supplied as

independent realizations using a multiple-realization analysis mode, allowing conditional independence tests to draw on observations from all phenotypes while respecting within-phenotype temporal order; for TE, lagged joint-probability estimates have been pooled across phenotypes without mixing observations across phenotype boundaries; and for CCM, because the climatic and socioeconomic drivers are identical across phenotypes within a given state-year, direct pooling into a single reconstructed manifold is not statistically valid (see Section 3.3.3), and phenotype-level results have been instead combined using Fisher's method for combining independent p-values (Fisher, 1932), in which the test statistic $-2\sum_{i=1}^{k} ln(p_i)$ follows a chi-squared distribution with $2k$ degrees of freedom under the null hypothesis of no association in any of the k pooled phenotypes.

Statistical significance has been assessed at the conventional threshold of $p < 0.05$, where the p-value denotes the probability of observing an association as strong as, or stronger than, the one detected if no true directional dependence existed between the driver and AMR (i.e., under the null hypothesis). Given the exploratory nature of causal discovery from short annual time series, associations in the range $0.05 \leq p < 0.1$ are additionally reported as suggestive/marginal signals, following standard practice for distinguishing primary from exploratory findings. Both nominal (uncorrected) and Benjamini-Hochberg false-discovery-rate (FDR)-adjusted (Benjamini and Hochberg, 1995) p-values have been reported for each threshold, given the large number of state-driver comparisons conducted. The multiple-testing family differs by method. For PCMCI, Benjamini–Hochberg correction has been applied within each state, across that state's candidate driver–lag tests (a state-specific family); for TE and CCM, it has been applied across all 196 state–driver tests. Because the PCMCI family is considerably smaller, its correction is less stringent than the global correction applied to TE and CCM, which partly explains why more associations survive for PCMCI (7 at FDR $p < 0.05$) than for CCM (1) or TE (0). As an additional robustness criterion, it has been highlighted that state-driver associations for which at least two of the three methods (PCMCI, TE, and CCM) independently indicated a significant association, since agreement across methods with distinct underlying assumptions provides stronger evidence than reliance on any single test. Pearson correlation coefficients have also been computed for descriptive purposes and have not been presented as statistical validation of causal findings.

3.3.1 Peter and Clark Momentary Conditional Independence (PCMCI)

PCMCI (Runge et al., 2019) is an algorithm developed to uncover causal linkages within multivariate time series data. This method is extensively utilized in the analysis of complex systems, especially in earth (Runge et al., 2019; Muszynski et al., 2026) and climate sciences (Krich et al., 2020; Docquier et al., 2024; Yeşilköy et al., 2026), and microbiome (Ruiz-Perez et al., 2024; Kardish et al., 2025).

The main target of PCMCI is to ascertain whether one variable affects another by eliminating spurious correlations and time-series-specific autocorrelation effects. PCMCI employs conditional independence testing to eliminate these spurious correlations. It

constitutes a two-stage methodology. Initially, potential parental relationships are determined by discarding superfluous links, including historical influences that do not directly impact the target variable, can be elucidated through other variables, or may induce misleading causation. In the subsequent stage, it establishes a significant causal network by the execution of conditional independence tests.

PCMCI has been implemented using the Tigramite Python package (Runge et al., 2019), with partial correlation (ParCorr) as the conditional independence test and a significance threshold of $pc_alpha = 0.05$ at the condition-selection stage. Given the annual, 14-year length of the underlying state-level series, the maximum time lag (τ_{max}) has been evaluated over the range 0–10; because higher lags leave progressively fewer usable year-to-year transitions per phenotype, τ_{max} has been capped at the largest value yielding non-degenerate conditional independence estimates, which in practice has been $\tau_{max} \leq 6$ for the pooled four-phenotype realizations.

3.3.2 Transfer Entropy (TE)

Based on the concepts of information theory, TE is a unique measure for measuring the transfer of information (Shannon, 1948). According to the original idea, entropy originates from the stationary probability of states, whereas the transition probabilities are used to determine the entropy rate. Based on the second idea, regardless of the historical data from Y, the transition probabilities of X stay unchanged when there is no information flow from Y to X (Sironen, 2020). Schreiber (2000) proposed employing Markov processes to approximate the two time series, $X = x_t$ and $Y = y_t$, and thereafter calculating the deviation from the generalized Markov condition as an indicator of causation, computed as the expected Kullback-Leibler divergence (Kullback, 1951) between the joint and conditionally independent probability distributions of the two series (Vicente et al., 2011).

TE has been implemented using a discretized (histogram-binned), plug-in entropy estimator, with each series divided into three bins and a lag of one year. Statistical significance has been assessed via a permutation-based surrogate test: the driver series has been randomly shuffled 150 times, TE has been recalculated for each shuffled realization to construct a null distribution, and the empirical p-value has been defined as (1 + the number of surrogate TE values equal to or exceeding the observed value) divided by (1 + the number of surrogates), following standard practice for avoiding zero p-values in permutation tests. Because surrogate testing uses the same (plug-in) estimator to construct both the observed and null distributions, systematic estimator bias is expected to largely cancel in the resulting significance assessment. As with PCMCI, the four resistance phenotypes have been pooled to increase the effective sample size: bin edges have been computed from the pooled distribution across all four phenotypes, after which lagged (present, own-history, driver-history) triplets have been extracted separately within each phenotype's 14-year series—ensuring no triplet spanned the boundary between two phenotypes—and combined into a single joint distribution for entropy estimation.

3.3.3 Convergent Cross Mapping (CCM)

CCM (Sugihara et al., 2012) is a nonlinear, state-space-based method (Baydaroğlu et al., 2025) for detecting causal coupling between time series, grounded in Takens' embedding theorem (Takens, 1981). Unlike PCMCI and TE, which rely on conditional-probability or information-theoretic dependence, CCM reconstructs the shadow manifold of a time series through time-delay embedding and tests whether the historical states of one variable can be recovered from the reconstructed manifold of another; convergence of cross-map skill with increasing library (time-series) length is taken as evidence of causal coupling, distinguishing it from mere correlation (Yeşilköy et al., 2026).

CCM has been implemented using the pyEDM Python package. For each phenotype, the optimal embedding dimension (E, tested over 1–5) and time delay (τ, tested over 1–7) have first been determined via simplex projection, selecting the combination maximizing self-prediction skill for the AMR series. The presence of nonlinearity, a prerequisite for meaningful CCM application, has then been assessed using the S-map method: if prediction skill has been maximized at a nonlinearity parameter of zero, the series has been treated as linear and excluded from CCM for that phenotype (relying instead on the PCMCI and TE results for that state-driver pair). Where nonlinearity has been confirmed, CCM has been applied using each phenotype's optimal (E, τ), with cross-map skill evaluated across increasing library sizes to assess convergence, and statistical significance assessed via a permutation-based surrogate test analogous to that used for TE (150 shuffles of the driver series).

As detailed in Section 3.3, because the climatic and socioeconomic drivers are identical across phenotypes within a given state-year, CCM cannot be validly pooled into a single reconstructed manifold: doing so causes the algorithm to match a given year in one phenotype to the identical year in another phenotype (owing to zero distance between their driver values), yielding cross-map skill estimates that are independent of which driver is tested. To address this while still leveraging information from all four phenotypes, CCM has instead been applied separately to each phenotype exhibiting nonlinear AMR dynamics, and the resulting (up to four) independent p-values have been combined using Fisher's method (Fisher, 1932), consistent with the approach described in Section 3.3.

4. Results

In brief, across all three methods and significance criteria, this study identifies one robust, three-method-consistent association (West Virginia–maximum temperature) and a further twelve state–driver pairs supported by at least two of the three methods at the nominal $p < 0.1$ level; no result survived FDR correction under cross-method agreement. The sections below present the single-method and consensus results underlying this summary in full detail.

Causal-discovery analyses have been conducted using the pooled four-phenotype framework described in Section 3.3, applying PCMCI, TE, and CCM in parallel across all

49 study states. For each state-driver pair, significance has been assessed at both $the\ p < 0.05$ and $p < 0.1$ levels, using both nominal (uncorrected) and Benjamini-Hochberg FDR-adjusted p-values, yielding four significance criteria that are reported jointly throughout this section. Results are presented as choropleth maps for each method, in which the dominant driver for each state—defined as the significant driver with the largest absolute effect size (partial correlation for PCMCI, information transfer for TE, cross-map skill for CCM)—is distinguished by color: green for PCPI, turquoise for precipitation, yellow for minimum temperature, and orange for maximum temperature. States where more than one driver is simultaneously significant are marked with an asterisk (*) next to their abbreviation. Full numerical results (effect sizes and nominal/FDR-adjusted p-values for all three methods and all four significance criteria) are given in Table 1. In addition, consensus maps are presented, highlighting state-driver pairs for which at least two of the three methods (or, more restrictively, all three methods) independently indicate significance, providing a cross-method robustness check as described in Section 3.3. Diagnostic plots underlying the CCM analysis (simplex projection, S-map nonlinearity tests, and cross-map convergence curves) are provided in the Appendix (Figures S1-6) rather than in the main text.

The TE score is an absolute value quantified in entropy units (bits), originating from information theory (Shannon, 1948), and assesses the directional flow and amount of information between two time series; a TE value of zero signifies the absence of information transfer, while a positive value implies information flow. The CCM cross-map skill (ρ) ranges from −1 to 1, with values approaching 1 indicating strong, convergent cross-map predictability consistent with causal coupling. For PCMCI, TE, and CCM alike, a driver–AMR association is classified as significant based solely on its p-value (nominal or FDR-adjusted) meeting the relevant threshold ($p < 0.05\ or\ p < 0.1$); no minimum magnitude of the underlying partial correlation, TE, or ρ value is required. Where more than one driver meets this significance criterion for a given state, the magnitude of the effect size is used only secondarily, to select which driver is displayed as the map's dominant color; all significant drivers, regardless of magnitude, are reported in full in Supplementary Table S2-S5.

4.1 Combined Cross-Method Overview

At the nominal ($p < 0.05$) threshold, PCMCI has identified 32 significant state–driver associations (of 196 possible; 49 states × 4 drivers), TE has identified 26, and CCM has identified 9; Pearson correlation, reported descriptively rather than as causal evidence, has identified 23. After FDR correction, the number of significant associations has fallen sharply for all three methods (PCMCI: 7; TE: 0; CCM: 1), reflecting the large number of comparisons conducted relative to the limited temporal depth of the underlying state-level series. At the more permissive $p < 0.1$ threshold, nominal associations have increased (PCMCI: 41; TE: 36; CCM: 17), while FDR-adjusted associations remained sparse (PCMCI: 12; TE: 0; CCM: 1).

Given the attenuation of single-method findings under FDR correction, cross-method agreement has been used as a complementary robustness criterion. At the stricter nominal $p < 0.05$ threshold, five state–driver pairs have met the two-of-three-methods consensus criterion: minimum temperature in Kansas (PCMCI+TE), Nebraska (PCMCI+TE), and Hawaii (PCMCI+TE); income in New York (PCMCI+CCM); and maximum temperature in West Virginia (TE+CCM) (Figure 3; Table 3); this set is a subset of the broader consensus obtained at $p < 0.1$, described below. At $p < 0.1$, thirteen state–driver pairs have been flagged as significant by at least two of the three methods (Tables 2 and 4, Figure 4): minimum temperature in six states (Hawaii, Iowa, Kansas, Montana, Nebraska, and New Mexico), income in five states (Georgia, Kansas, New York, Ohio, and Oklahoma), precipitation in Kansas, and maximum temperature in West Virginia (uniquely supported by all three methods). Kansas is the only state at which three distinct drivers—income, precipitation, and minimum temperature—each independently met the two-of-three-method consensus criterion and is marked with an asterisk in Figure 4 accordingly. A single state–driver pair—West Virginia and maximum temperature—has been independently identified as significant by all three methods (PCMCI, TE, and CCM) at $p < 0.1$, representing the most robust finding of this study (Figure 5; Table 5). Notably, none of the FDR-adjusted results showed cross-method agreement, underscoring that even this consensus-based finding should be interpreted as a robust nominal signal rather than one surviving the most conservative correction. Because TE relies on permutation-based surrogate testing, associations near the significance boundary (e.g., several minimum- and maximum-temperature associations in this section) showed minor sensitivity to the stochastic surrogate draw across independent runs; the West Virginia–maximum temperature consensus finding remained stable across runs.

The three methods probe different lag structures (PCMCI: lags 0 to τ_{max}, here lag 4 for West Virginia; TE: a fixed 1-year lag; CCM: embedding-based), so the three-method consensus does not imply agreement on a common lag.

Table 1. Summary of significant state–driver associations by method and significance criterion. Values indicate the number of significant state–driver pairs (out of 196 possible: 49 states × 4 drivers) for each method.

Significance Criterion	PCMCI	TE	CCM	Corr (descriptive)
Nominal, $p < 0.05$	32	26	9	23
FDR-adjusted, $p < 0.05$	7	0	1	1
Nominal, $p < 0.1$	41	36	17	43
FDR-adjusted, $p < 0.1$	12	0	1	2

Table 2. Cross-method consensus: state–driver associations independently identified as significant (nominal $p < 0.1$) by two or more of the three causal-discovery methods. The single pair identified by all three methods (West Virginia – Max. Temperature) is shown in bold with yellow shading.

State	Driver	Agreeing Methods	Agreement Level
Georgia	PCPI	TE + CCM	Two of three methods
Kansas	PCPI	PCMCI + TE	Two of three methods
New York	PCPI	PCMCI + CCM	Two of three methods
Ohio	PCPI	TE + CCM	Two of three methods
Oklahoma	PCPI	PCMCI + TE	Two of three methods
Kansas	Precipitation	PCMCI + TE	Two of three methods
Nebraska	Min. Temperature	PCMCI + TE	Two of three methods
West Virginia	**Max. Temperature**	**PCMCI + TE + CCM**	**All three methods**
Hawaii	Min. Temperature	PCMCI + TE	Two of three methods
Iowa	Min. Temperature	PCMCI + CCM	Two of three methods
Kansas	Min. Temperature	PCMCI + TE	Two of three methods
Montana	Min. Temperature	PCMCI + TE	Two of three methods
New Mexico	Min. Temperature	PCMCI + TE	Two of three methods

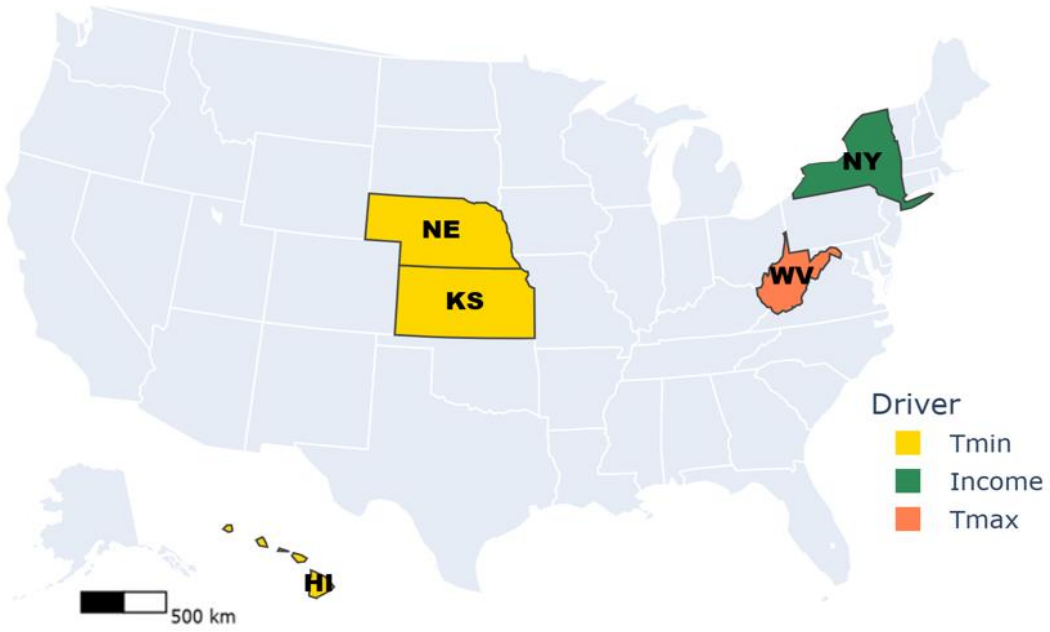


Figure 3. States with at least two of three methods (PCMCI, TE, CCM) indicating a significant driver–AMR association at nominal $p < 0.05$. Color denotes the agreed-upon dominant driver.

Table 3. Driver-level PCMCI, TE, and CCM values for the five state–driver pairs meeting the two-of-three-method consensus criterion at nominal $p < 0.05$ (Figure 3). Only PCMCI

values carry directional meaning (positive = positive partial correlation, negative = negative/inverse partial correlation). TE values are non-negative by construction (Section 3.3.2) and indicate the magnitude of information transfer only, not its direction; CCM values (ρ) indicate cross-map prediction skill and should not be interpreted as a signed directional coefficient in the same sense as PCMCI's partial correlation.

Drivers	**PCPI**			**Precipitation**			**Max. Temperature**			**Min. Temperature**		
Methods States	PCMCI	TE	CCM	PCMCI	TE	CCM	PCMCI	TE	CCM	PCMCI	TE	CCM
Hawaii	x	x	x	0.57	x	x	x	x	x	0.58	0.32	x
Kansas	0.53	x	x	0.61	x	x	x	0.38	x	0.46	0.41	x
Nebraska	x	x	x	x	0.21	x	-0.59	x	x	-0.65	0.18	x
New York	0.59	x	0.37	x	0.25	x	x	x	x	x	x	x
West Virginia	x	0.38	x	x	0.34	x	x	0.38	0.51	x	0.38	x

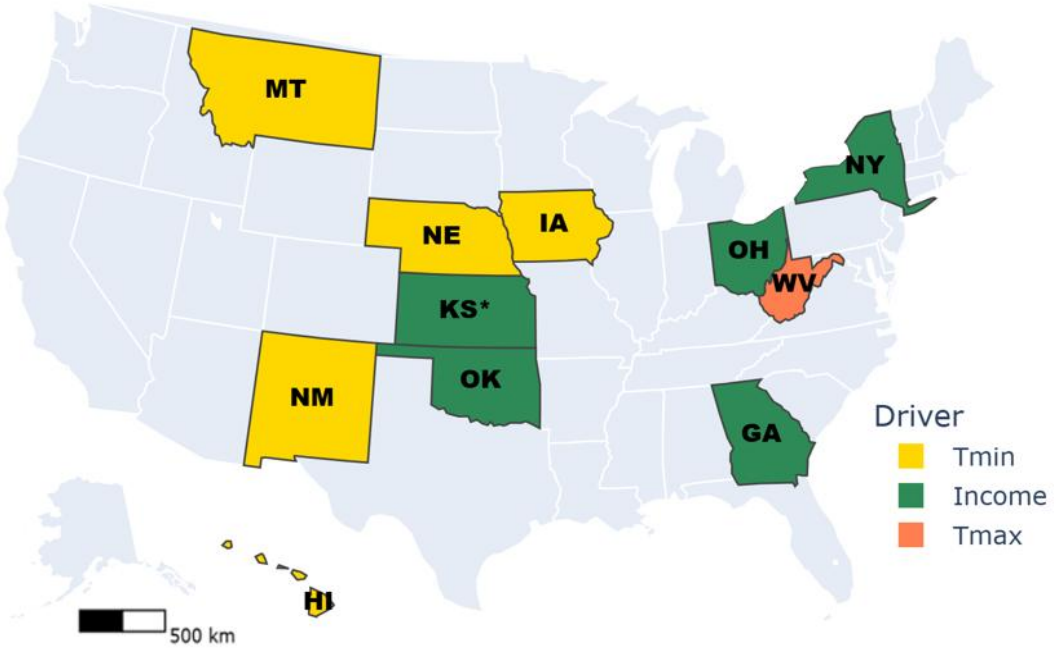


Figure 4. States with at least two of three methods (PCMCI, TE, CCM) indicating a significant driver–AMR association at nominal $p < 0.1$. Color denotes the agreed-upon dominant driver; an asterisk indicates more than one driver met this criterion in that state.

Table 4. Driver-level PCMCI, TE, and CCM values for the thirteen state–driver pairs meeting the two-of-three-method consensus criterion at nominal $p < 0.1$ (Figure 4). Only PCMCI values carry directional meaning (positive = positive partial correlation, negative = negative/inverse partial correlation). TE values are non-negative by construction (Section 3.3.2) and indicate the magnitude of information transfer only, not its direction; CCM values (ρ) indicate cross-map prediction skill and should not be interpreted as a signed directional coefficient in the same sense as PCMCI's partial correlation.

Drivers	PCPI			Precipitation			Max. Temperature			Min. Temperature		
Methods / **States**	PCMCI	TE	CCM	PCMCI	TE	CCM	PCMCI	TE	CCM	PCMCI	TE	CCM
Georgia	x	0.19	-0.06	x	x	x	x	x	x	x	x	x
Hawaii	x	x	x	0.57	x	x	x	x	x	0.58	0.32	x
Iowa	-0.71	x	x	0.63	x	x	x	x	x	-0.68	x	0.10
Kansas	0.53	0.29	x	0.61	0.29	x	x	0.38	x	0.46	0.41	x
Montana	0.54	x	x	x	x	x	x	x	x	-0.55	0.29	x
Nebraska	x	x	x	x	0.21	x	-0.59	x	x	-0.65	0.18	x
New Mexico	x	x	x	x	x	x	x	x	x	0.59	0.19	x
New York	0.59	x	0.37	x	0.25	x	x	x	x	x	x	x
Ohio	x	0.37	-0.01	x	x	x	0.627	x	x	x	x	x
Oklahoma	0.41	0.31	x	x	x	x	x	x	x	-0.39	x	x
West Virginia	x	0.38	x	x	0.34	x	0.40	0.38	0.51	x	0.38	x



Figure 5. The single state–driver pair (West Virginia – maximum temperature) independently identified as significant by all three methods (PCMCI, TE, and CCM) at nominal $p < 0.1$, representing the most robust finding of this study.

Table 5. Driver-level PCMCI, TE, and CCM values for West Virginia, the sole state–driver pair meeting the three-of-three-method consensus criterion (Figure 5).

Drivers	PCPI			Precipitation			Max. Temperature			Min. Temperature		
Methods / **States**	PCMCI	TE	CCM	PCMCI	TE	CCM	PCMCI	TE	CCM	PCMCI	TE	CCM
West Virginia	x	x	x	x	x	x	0.40	0.38	0.51	x	x	x

Full results for all 49 states (including those not meeting the two-of-three-method consensus criterion) are provided in Tables S2–S5.

4.2 PCMCI Results

Although PCMCI has been configured to evaluate lags up to $\tau = 10$ years, the maximum lag actually tested per state has been adaptively capped at the largest value yielding non-degenerate conditional-independence estimates; in practice this is $\tau = 4$ for 14 states, $\tau = 5$ for 33 states, and $\tau = 6$ for 2 states, with $\tau_{min} = 0$ (contemporaneous) has included in all cases.

Driver-level results for PCMCI are summarized in Table 1 (Section 4.1) and mapped in Figures 6–9 (nominal $p < 0.05$, FDR $p < 0.05$, nominal $p < 0.1$, and FDR $p < 0.1$, respectively). At the nominal $p < 0.05$ threshold, significant associations have been broadly distributed across drivers, with maximum and minimum temperature each accounting for 7 of the 32 significant state–driver pairs, PCPI for 5, and precipitation for 2 (21 states in total; Figure 6, Table 6).

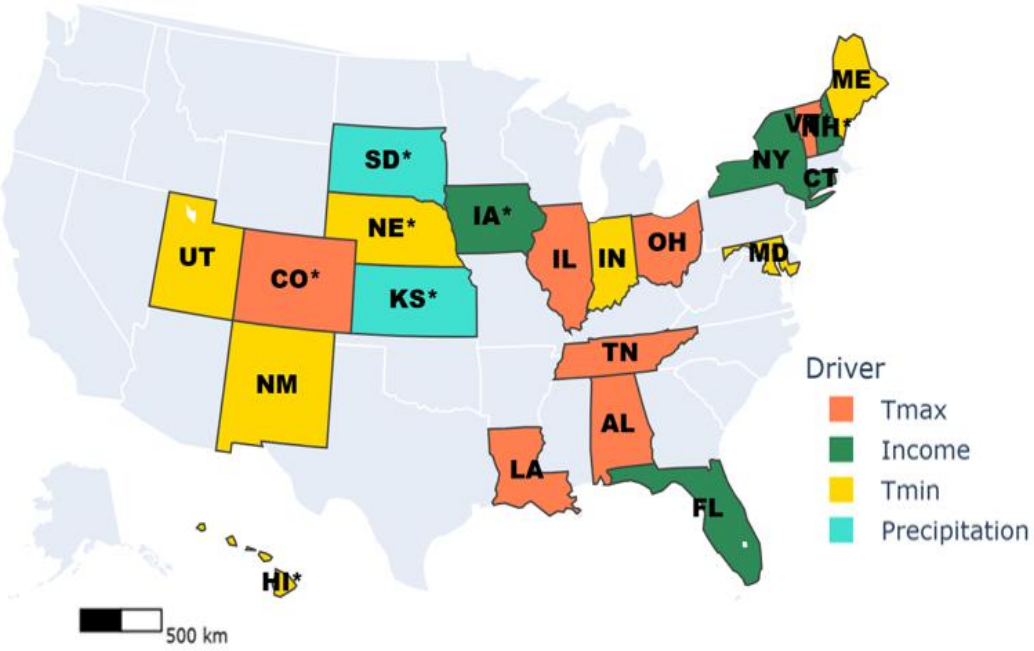


Figure 6. PCMCI dominant drivers by state at the nominal p < 0.05. Color denotes the driver with the largest absolute partial correlation for each significant state; an asterisk indicates more than one driver is significant in that state.

Table 6. PCMCI partial-correlation values by state and driver at the nominal $p < 0.05$ threshold (Figure 6).

Drivers States	PCPI	Precipitation	Max. Temperature	Min. Temperature
Alabama			0.53	
Colorado			0.65	-0.46
Connecticut	0.52			
Florida	-0.55			
Hawaii		0.57		0.58

Illinois			0.88	
Indiana				-0.67
Iowa	-0.71	0.63		-0.68
Kansas	0.53	0.61		0.46
Louisiana			0.65	
Maine				0.63
Maryland				-0.67
Nebraska			-0.59	-0.65
New Hampshire	-0.51			0.51
New Mexico				0.59
New York	0.59			
Ohio			0.63	
South Dakota		-0.80	-0.65	0.73
Tennessee			-0.52	
Utah				-0.72
Vermont	0.72		0.96	

Under FDR correction, this reduced to 7 pairs across 5 states: maximum temperature in Colorado, Illinois, and Vermont; minimum temperature in Nebraska; and, uniquely, three concurrently significant drivers (precipitation, minimum temperature, and maximum temperature) in South Dakota (Figure 7; Table 7). At the more permissive nominal $p < 0.1$ threshold, the pattern is similar but broader (41 pairs, 26 states; Figure 8, Table 8), while FDR correction at this threshold has retained 12 pairs across 7 states (Figure 9; Table 9).

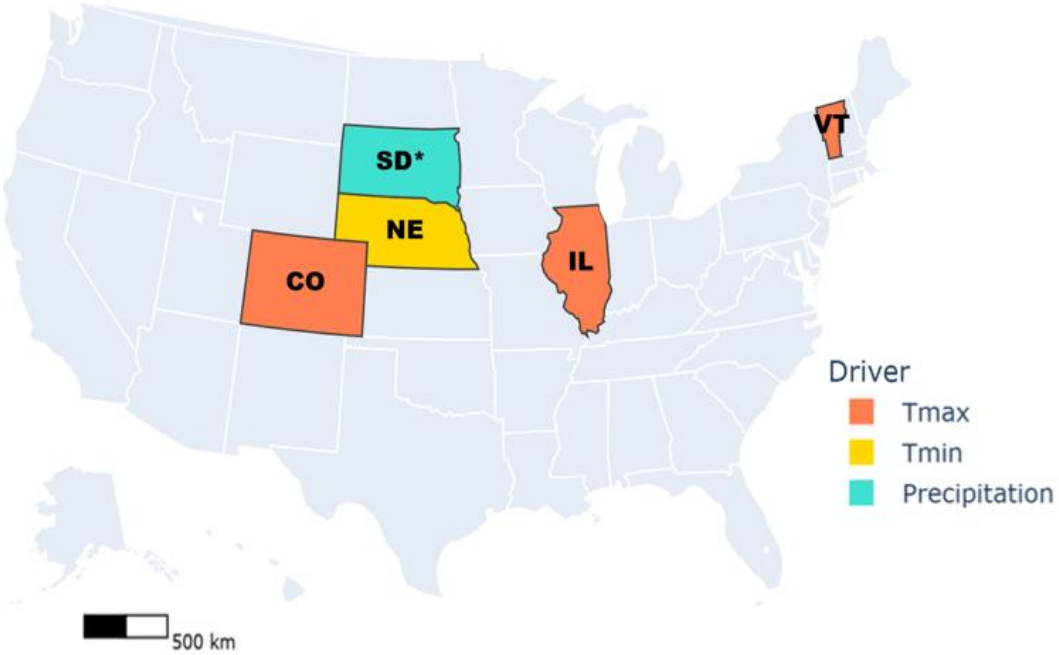


Figure 7. PCMCI dominant drivers by state, restricted to associations surviving FDR correction at $p < 0.05$.

Table 7. PCMCI partial-correlation values by state and driver surviving FDR correction at $p < 0.05$ (Figure 7).

Drivers / States	PCPI	Precipitation	Max. Temperature	Min. Temperature
Colorado			0.65	
Illinois			0.86	
Nebraska				-0.65
South Dakota		-0.80	-0.65	0.73
Vermont			0.96	

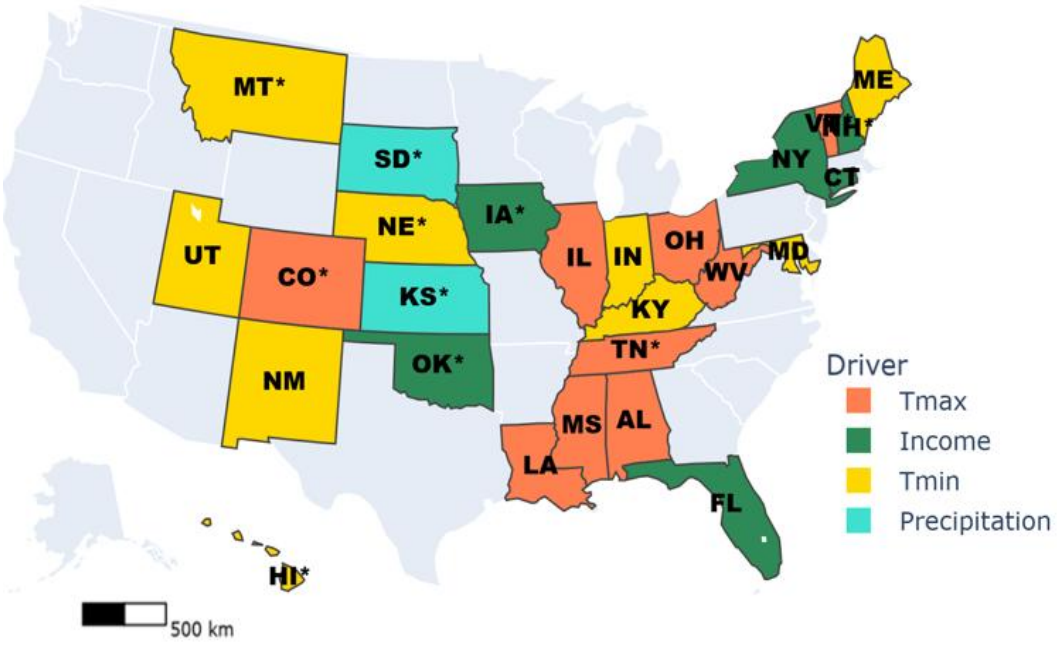


Figure 8. PCMCI dominant drivers by state at the nominal $p < 0.1$ threshold.

Table 8. PCMCI partial-correlation values by state and driver at the nominal $p < 0.1$ threshold (Figure 8).

Drivers / States	PCPI	Precipitation	Max. Temperature	Min. Temperature
Alabama			0.53	
Colorado			0.65	-0.46
Connecticut	0.52			
Florida	-0.55			
Hawaii		0.57		0.58
Illinois			0.88	
Indiana				-0.67
Iowa	-0.71	0.63		-0.68
Kansas	0.53	0.61		0.46

Kentucky				-0.48
Louisiana			0.65	
Maine				0.63
Maryland				-0.67
Mississippi			0.48	
Montana	0.54			-0.55
Nebraska			-0.59	-0.65
New Hampshire	-0.51		-0.46	0.51
New Mexico				0.59
New York	0.59			
Ohio			0.63	
Oklahoma	0.41			-0.39
South Dakota		-0.80	-0.65	0.73
Tennessee			-0.52	-0.39
Utah				-0.72
Vermont	0.72		0.96	
West Virginia			0.40	

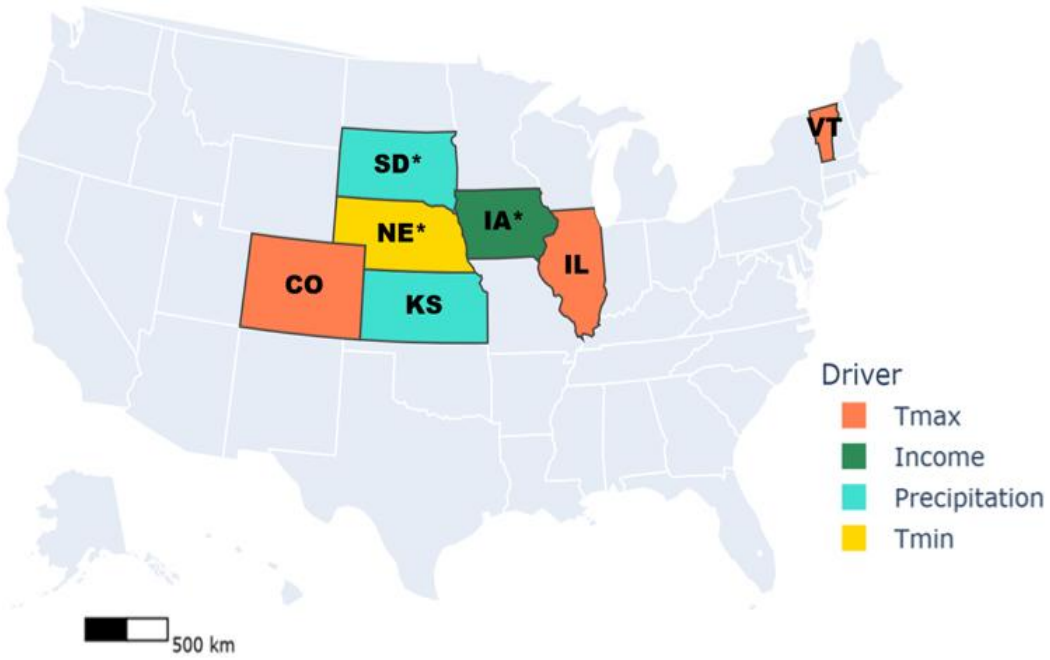


Figure 9. PCMCI dominant drivers by state, restricted to associations surviving FDR correction at $p < 0.1$.

Table 9. PCMCI partial-correlation values by state and driver surviving FDR correction at $p < 0.1$ (Figure 9).

Drivers / States	PCPI	Precipitation	Max. Temperature	Min. Temperature

Colorado			0.65	
Illinois			0.88	
Iowa	-0.71	0.63		-0.68
Kansas		0.61		
Nebraska			-0.59	-0.65
South Dakota		-0.80	-0.65	0.73
Vermont			0.96	

The twelve state–driver pairs surviving FDR correction at $p < 0.1$ are listed in Table 10. Ten of these twelve associations have occurred at a time lag of 0–2 years, with only one (Iowa–PCPI) at a longer lag (5 years), suggesting that where PCMCI detects a robust signal, the climatic or economic driver tends to precede the observed change in AMR by a relatively short interval. Across all associations significant at the nominal p < 0.05 threshold, the majority (26 of 32) has occurred at a non-zero lag (i.e., the driver has preceded AMR by one or more years) rather than contemporaneously, consistent with a delayed rather than instantaneous relationship between climatic/economic conditions and resistance levels. Effect directions have been mixed: of the 32 nominally significant associations, 19 have been positive and 13 have been negative, indicating that the sign of the driver–AMR relationship is state- and driver-specific rather than uniform across the study area.

The four significance criteria in Table 1 (nominal/FDR-adjusted, $p < 0.05/0.1$) represent thresholds used to count associations meeting each level of evidence; Table 10 indicates the underlying, continuously varying nominal and FDR-adjusted p-values for the twelve associations meeting the most permissive of these criteria (FDR-adjusted $p < 0.1$).

Table 10. State–driver associations surviving FDR correction at nominal $p < 0.1$. Lag denotes the number of years by which the driver precedes AMR. Positive PCMCI values indicate a positive partial correlation; negative values indicate a negative (inverse) association. Identical FDR-adjusted p-values across multiple rows for the same state (e.g., Iowa) arise from the monotonicity constraint of the Benjamini-Hochberg procedure, under which adjusted p-values cannot decrease as raw p-value rank increases within the state-specific test family.

State	Driver	Lag (years)	PCMCI Value	Nominal p	FDR-adjusted p
Illinois	Max. Temperature	2	0.88	<0.001	0.002
South Dakota	Precipitation	1	-0.80	<0.001	0.002
South Dakota	Min. Temperature	2	0.73	0.001	0.007
South Dakota	Max. Temperature	1	-0.65	0.003	0.017

Vermont	Max. Temperature	1	0.96	0.001	0.003
Colorado	Max. Temperature	0	0.65	0.001	0.020
Nebraska	Min. Temperature	1	-0.65	0.002	0.030
Nebraska	Max. Temperature	1	-0.59	0.006	0.059
Kansas	Precipitation	1	0.61	0.004	0.072
Iowa	Min. Temperature	0	-0.68	0.01	0.080
Iowa	PCPI	5	-0.71	0.005	0.080
Iowa	Precipitation	2	0.63	0.022	0.080

For West Virginia—the state identified as significant across all three methods for maximum temperature (Section 4.1)—the PCMCI association itself has been positive at a lag of 4 years (nominal p = 0.077), meeting the p < 0.1 but not the p < 0.05 threshold, and not surviving FDR correction (adjusted p = 0.945) when considered in isolation; its significance in this study rests on the convergence of independent evidence from TE and CCM rather than on the strength of the PCMCI result alone.

4.3 Transfer Entropy Results

TE results are summarized in Table 1 and mapped in Figures 10–11 (detailed in Tables 11–12) (nominal $p < 0.05$ and $p < 0.1$, respectively); no FDR-adjusted maps are shown, as no state–driver pair survived FDR correction at either threshold (the lowest FDR-adjusted p-value obtained across all 196 tests was 0.162). At the nominal $p < 0.05$ threshold, 26 significant state–driver pairs have been identified across 20 states, most frequently involving precipitation (10 pairs), minimum temperature (7), PCPI (5), and maximum temperature (4). At the more permissive nominal $p < 0.1$ threshold, this has increased to 36 pairs across 25 states, with a similar ordering (precipitation: 15; minimum temperature: 9; PCPI: 8; maximum temperature: 4). In contrast to PCMCI, which has frequently identified maximum and minimum temperatures as the primary drivers, TE has most often identified precipitation as a significant factor, suggesting that the two methods are sensitive to different aspects of the driver–AMR relationship.

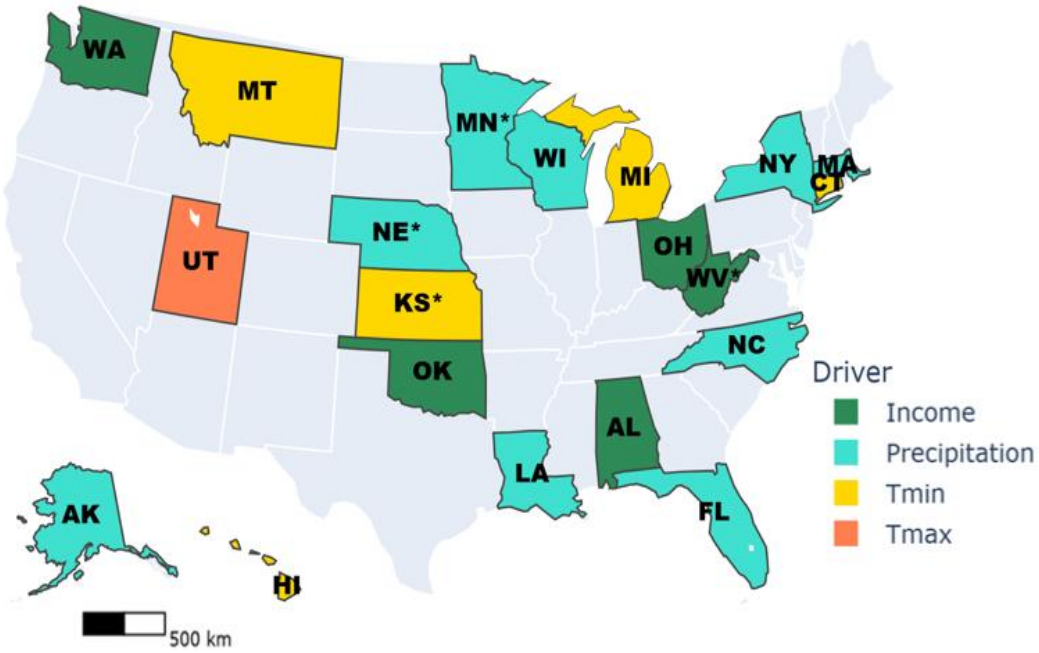


Figure 10. TE dominant drivers by state at the nominal $p < 0.05$ threshold. Color denotes the driver with the largest TE value meeting this threshold in each state; an asterisk indicates more than one driver met this criterion in that state.

Table 11. TE values by state and driver at the nominal $p < 0.05$ threshold (Figure 10).

Drivers States	PCPI	Precipitation	Max. Temperature	Min. Temperature
Alabama	0.41			
Alaska		0.42		
Connecticut				0.30
Florida		0.27		
Hawaii				0.32
Kansas			0.38	0.41
Louisiana		0.24		
Massachusetts		0.34		
Michigan				0.27
Minnesota		0.32	0.30	
Montana				0.29
Nebraska		0.21		0.18
New York		0.25		
North Carolina		0.20		
Ohio	0.37			
Oklahoma	0.31			
Utah			0.24	
Washington	0.32			
West Virginia	0.38	0.34	0.38	0.38
Wisconsin		0.29		

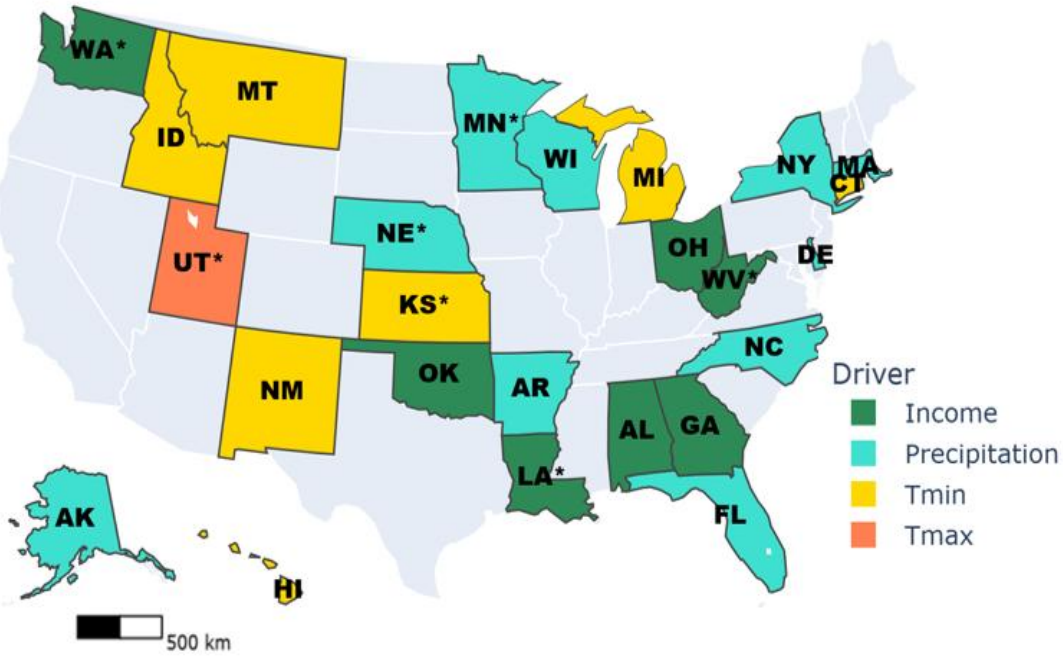


Figure 11. TE dominant drivers by state at the nominal $p < 0.1$ threshold.

Table 12. TE values by state and driver at the nominal $p < 0.1$ threshold (Figure 11).

Drivers States	PCPI	Precipitation	Max. Temperature	Min. Temperature
Alabama	0.41			
Alaska		0.42		
Arkansas		0.30		
Connecticut				0.30
Delaware		0.25		
Florida		0.27		
Georgia	0.19			
Hawaii				0.32
Idaho				0.26
Kansas	0.29	0.29	0.38	0.41
Louisiana	0.33	0.24		
Massachusetts		0.34		
Michigan				0.27
Minnesota		0.32	0.30	
Montana				0.29
Nebraska		0.21		0.18
New Mexico				0.19
New York		0.25		
North Carolina		0.20		

Ohio	0.37			
Oklahoma	0.31			
Utah		0.22	0.24	
Washington	0.32	0.31		
West Virginia	0.38	0.34	0.38	0.38
Wisconsin		0.29		

Because TE significance has been assessed via a permutation-based surrogate test with 150 shuffles, the smallest attainable p-value is bounded at 1/151 ≈ 0.0066; eight state–driver pairs reached this floor, including West Virginia–maximum temperature ($TE = 0.379$, $p = 0.0066$), consistent with, and reinforcing, its identification as the sole pair significant across all three methods. West Virginia's PCPI and minimum-temperature associations have also reached this floor, suggesting that AMR dynamics in this state are informationally coupled with multiple climatic and socioeconomic drivers rather than maximum temperature alone; this pattern is explored further in the Discussion.

As with PCMCI, the complete absence of FDR-surviving associations for TE—more pronounced than for PCMCI or CCM (Table 1)—reflects the large number of comparisons (196 per threshold) relative to the statistical power attainable from 14-year annual state-level series, even after pooling across four phenotypes. This reinforces the interpretation, developed in Section 4.1, that nominal-level TE associations should be treated as candidate signals for further investigation rather than confirmed findings.

4.4 Convergent Cross Mapping Results

As described in Section 3.3.3, AMR nonlinearity has been assessed once per state–phenotype combination via the S-map test (196 tests: 49 states × 4 phenotypes), independent of the driver under consideration, since this property depends only on the AMR series itself. For a given state, the same set of phenotypes confirmed as nonlinear has been subsequently used in CCM testing against all four drivers. Across the 49 states, all four phenotypes have been classified as nonlinear (and thus CCM-eligible—i.e., meeting both the minimum data-availability criterion described in Section 3.1 and the confirmed-nonlinearity criterion applied here) in 25 states, three phenotypes in 19 states, and two phenotypes in the remaining 5 states; no state has fewer than two CCM-eligible phenotypes, indicating that nonlinear AMR dynamics are common rather than exceptional across the dataset. For each state–driver pair, CCM has been then applied separately to each CCM-eligible phenotype, with the resulting phenotype-level p-values combined via Fisher's method.

Because the underlying annual series span 14 years, CCM library sizes are correspondingly small (maximum library size = 14); convergence has been assessed by examining the trend across the full range of tested library sizes (4–14) rather than at a single value, following standard CCM practice, though the narrow range of library sizes tested—an inherent constraint of the 14-year annual series—limits the resolving power of

this convergence assessment relative to typical CCM applications using substantially longer libraries.

CCM results are summarized in Table 1 and mapped in Figures 12–15 (nominal $p < 0.05$, FDR $p < 0.05$, nominal $p < 0.1$, and FDR $p < 0.1$, respectively). At the nominal $p < 0.05$ threshold, 9 significant state–driver pairs have been identified across 8 states, most frequently involving PCPI (6 pairs), maximum temperature (2), and minimum temperature (1) (Figure 12; Table 13). At the nominal $p < 0.1$ threshold, this increased to 17 pairs across 13 states, with PCPI remaining dominant (10 pairs), followed by maximum temperature (4), minimum temperature (2), and precipitation (1) (Figure 14; Table 15). Unlike PCMCI and TE, for which temperature-related drivers have most frequently been implicated, CCM most often identified PCPI, a third point of divergence across the three methods.

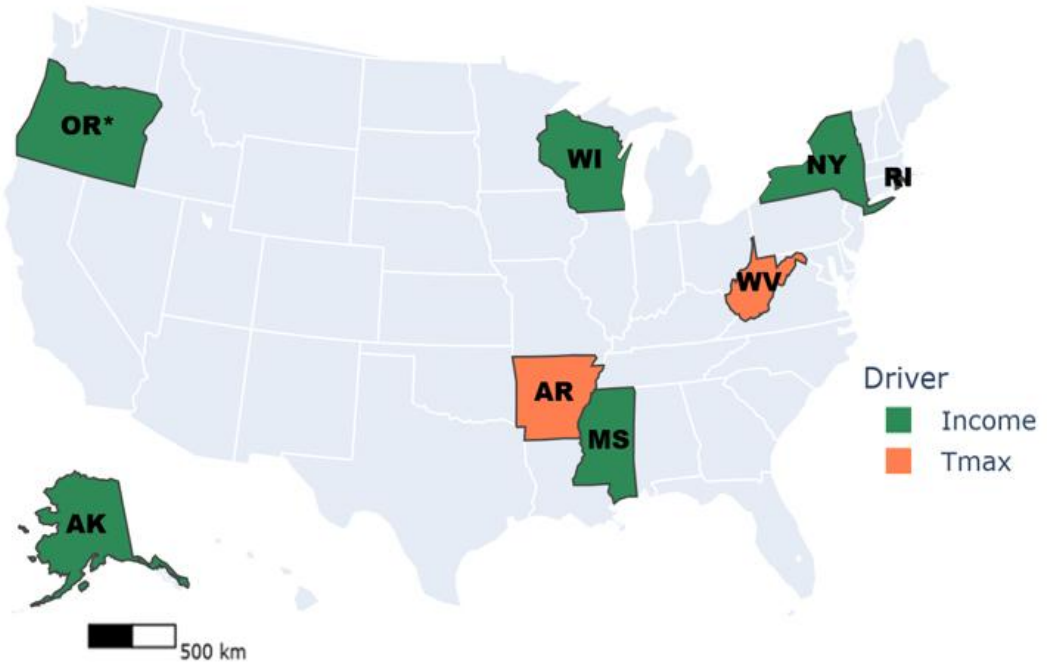


Figure 12. CCM dominant drivers by state at the nominal $p < 0.05$ threshold. Color denotes the driver with the largest mean cross-map skill meeting this threshold in each state; an asterisk indicates more than one driver met this criterion in that state.

Table 13. CCM cross-map skill (mean ρ) values by state and driver at the nominal $p < 0.05$ threshold (Figure 12).

Drivers / States	PCPI	Precipitation	Max. Temperature	Min. Temperature
Alaska	0.10			
Arkansas			0.05	
Mississippi	0.01			
New York	0.37			

Oregon	0.37			0.16
Rhode Island	0.26			
West Virginia			0.51	
Wisconsin	0.21			



Figure 13. CCM dominant drivers by state, restricted to associations surviving FDR correction at $p < 0.05$.

Table 14. CCM cross-map skill (mean ρ) values by state and driver surviving FDR correction at $p < 0.05$ (Figure 13).

Drivers / States	PCPI	Precipitation	Max. Temperature	Min. Temperature
West Virginia			0.51	

Only a single state–driver pair—West Virginia and maximum temperature—survived FDR correction, at both the $p < 0.05$ and $p < 0.1$ thresholds alike (Figures 13 and 15; Tables 14 and 16), indicating that this result is not sensitive to the choice between the two threshold levels. This association is also the strongest observed in the CCM analysis (mean cross-map skill $\rho = 0.509$; Fisher-combined $p < 0.001$; FDR-adjusted $p = 0.038$) and is supported individually by all four resistance phenotypes (MDR: $\rho = 0.635$, $p = 0.007$; carbapenem-resistant: $\rho = 0.446$, $p = 0.013$; cephalosporin-resistant: $\rho = 0.383$, $p = 0.079$; fluoroquinolone-resistant: $\rho = 0.574$, $p = 0.040$), each showing a positive cross-map skill. This consistency across all four separetely tested phenotypes, combined with the fact that this is the only CCM association to survive FDR correction on its own—independent of the cross-method consensus criterion used in Section 4.1—

provides the strongest single piece of evidence in this study for a directional association between maximum temperature and *E. coli* AMR, specific to West Virginia.

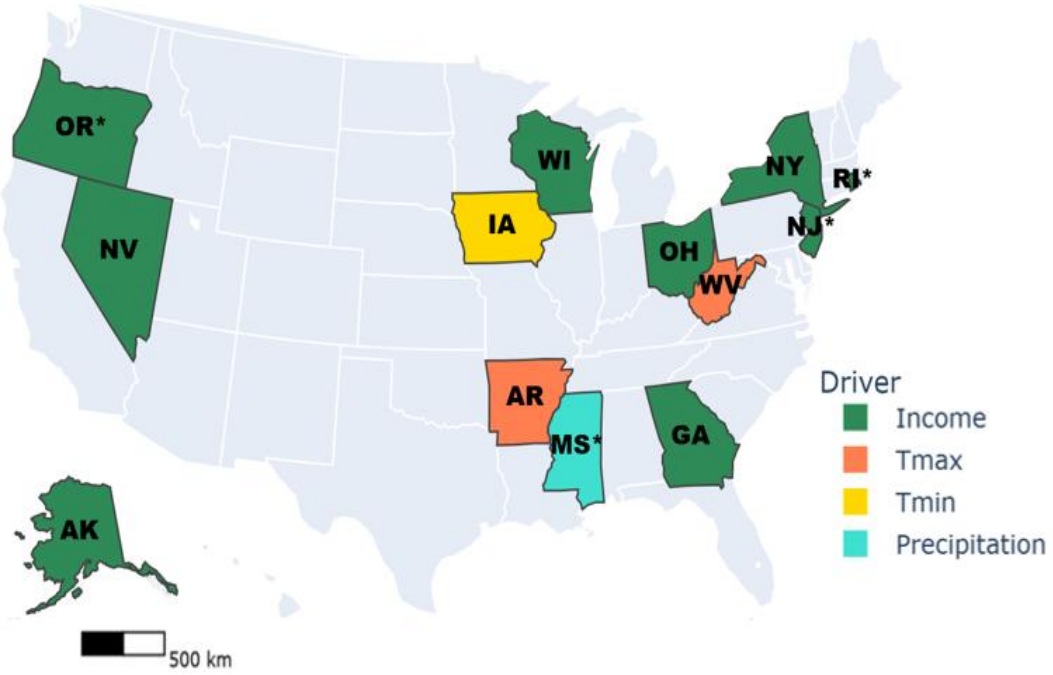


Figure 14. CCM dominant drivers by state at the nominal $p < 0.1$ threshold.

Table 15. CCM cross-map skill (mean ρ) values by state and driver at the nominal $p < 0.1$ threshold (Figure 14).

Drivers States	PCPI	Precipitation	Max. Temperature	Min. Temperature
Alaska	0.10			
Arkansas			0.05	
Georgia	-0.06			
Iowa				0.10
Mississippi	0.01	0.17		
Nevada	0.22			
New Jersey	0.11		-0.03	
New York	0.37			
Ohio	-0.01			
Oregon	0.37			0.16
Rhode Island	0.26		0.15	
West Virginia			0.51	
Wisconsin	0.21			

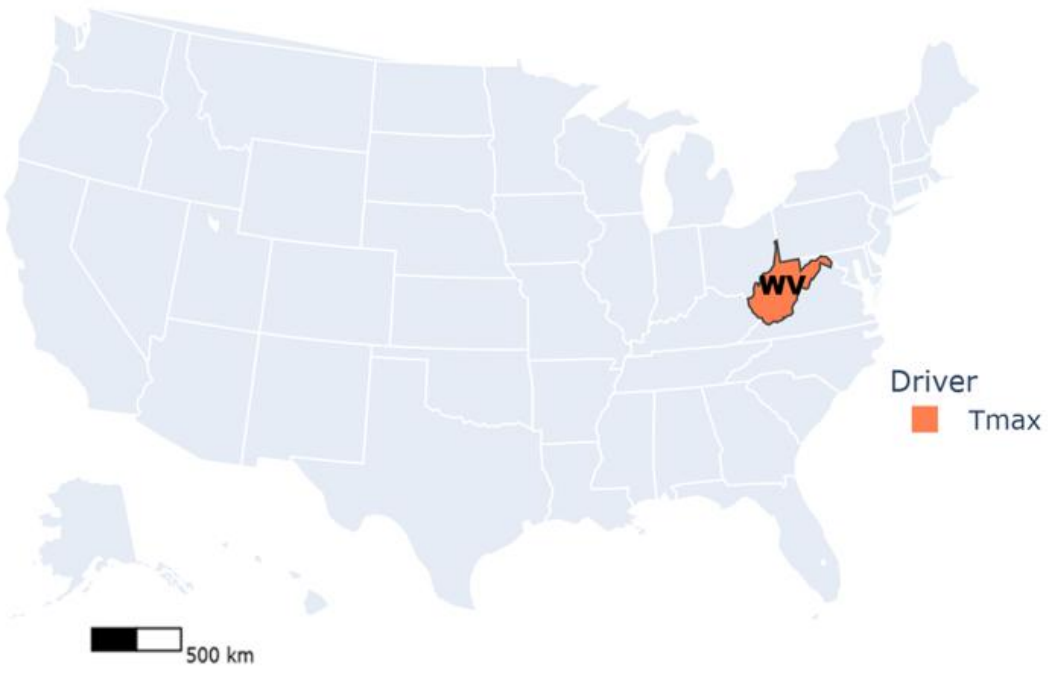


Figure 15. CCM dominant drivers by state, restricted to associations surviving FDR correction at $p < 0.1$.

Table 16. CCM cross-map skill (mean ρ) values by state and driver surviving FDR correction at $p < 0.1$ (Figure 15).

Drivers / States	PCPI	Precipitation	Max. Temperature	Min. Temperature
West Virginia			0.51	

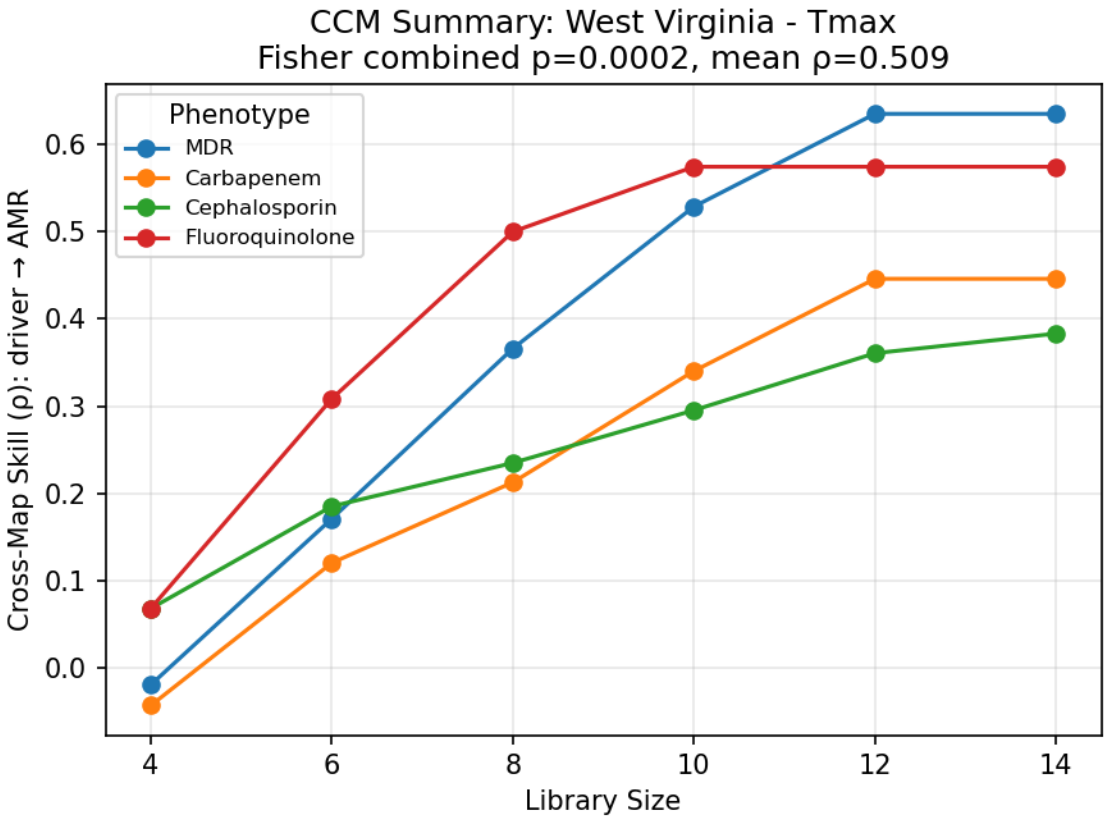


Figure 16. Cross-map skill as a function of library size for the West Virginia–maximum temperature association, shown separately for each of the four resistance phenotypes. All four phenotypes exhibit an increasing and converging cross-map skill as library size increases, which is the classic signature of CCM convergence within the tested library-size range, aligning with the Fisher-combined significance reported above.

Diagnostic plots underlying these CCM results (simplex projection and S-map nonlinearity tests for each phenotype) are provided in the Appendix (Figures S1–S6); the cross-map convergence summary for the West Virginia–maximum temperature association is shown above (Figure 16), with representative non-significant and non-convergent examples provided for comparison in the Appendix.

5. Discussions

5.1 Findings in the context of existing literature

The associations identified in this study are broadly consistent with, while adding spatial and temporal specificity to, the existing literature linking climatic and socioeconomic conditions to AMR. The positive association between maximum temperature and AMR has been observed in West Virginia—the only association supported independently by all three causal-discovery methods and the only CCM association surviving FDR correction—aligns directionally with experimental evidence that elevated growth temperatures accelerate the emergence of antibiotic-resistance mutations in *E. coli*

(Rodríguez-Verdugo et al., 2020) and with observational work linking ambient temperature to elevated resistance at regional scale (Kou et al., 2025; Kalanxhi and Laxminarayan, 2026). More broadly, minimum temperature and PCPI have been the drivers most frequently implicated in the thirteen state–driver pairs meeting the two-of-three-method consensus criterion at $p < 0.1$ (Section 4.1), a pattern consistent with reports that both temperature extremes and socioeconomic conditions—rather than mean climatic exposure alone—shape AMR dynamics (Ljungqvist et al., 2025; Wang et al., 2025). The relatively frequent implication of precipitation by TE specifically (Section 4.3) is also consistent with proposed pathways through which rainfall disseminates resistance genes via wastewater and agricultural runoff (Kalanxhi and Laxminarayan, 2026; Booth and Wester, 2022). At the same time, the present findings differ from this literature in an important respect: whereas prior studies have generally reported associations as established correlates or, in some cases, as causal mechanisms, the present results—after correction for multiple testing—identify only a small number of associations meeting a comparable standard of statistical robustness, underscoring that state-level annual surveillance data of the kind available for this study offer considerably less statistical power than the multi-country or high-resolution genomic datasets used in much of the cited work.

For ease of reference, Table 2 is summarized graphically in Figure 4, which shows all thirteen state–driver pairs meeting the two-of-three-method consensus criterion on a single map; readers seeking single-method detail (e.g., which additional driver is significant for a starred state) should consult Table 2 for the ≥2-method associations and the full state-by-driver results (Table S2-S5) for single-method findings shown in Figures 6–15.

5.2 Why the three methods diverge in their most frequently implicated drivers

A notable pattern across Sections 4.2–4.4 is that the three causal-discovery methods, while converging on a single association (West Virginia–maximum temperature), diverged in which driver they most frequently implicated overall: temperature extremes for PCMCI, precipitation for TE, and PCPI for CCM. This divergence has not been tested directly, and offer the following as a plausible, untested hypothesis for future investigation rather than a confirmed explanation. PCMCI, TE, and CCM differ fundamentally in the statistical structure they are designed to detect—linear partial correlation conditional on a fixed lag structure; information-theoretic transfer, which is sensitive to any statistical dependence regardless of functional form; and nonlinear state-space reconstruction, which specifically requires and exploits deterministic nonlinear dynamics. If the true relationship between a given driver and AMR differs in functional form across drivers (for example, if temperature effects are more linear and lagged, while precipitation effects are more information-rich but less deterministic, and income effects are more strongly nonlinear), each method would be expected to preferentially detect the driver whose relationship with AMR best matches its own statistical assumptions. Under this

hypothesis, the three methods are not competing estimates of a single "true" dominant driver but complementary probes of different aspects of a genuinely multivariate and possibly multi-mechanism system—reinforcing the value of the multi-method, consensus-based approach adopted here, rather than reliance on any single method.

5.3 Possible mechanisms underlying the West Virginia finding

The consistency of the West Virginia–maximum temperature association across all three methods and all four resistance phenotypes (Section 4.4) makes it the most robust single result of this study, but the present analysis has not been designed to, and does not, identify the mechanism underlying it. The following untested hypotheses are offered that could motivate future, state-specific investigation, rather than as explanations supported by this study's data. West Virginia is characterized by a predominantly rural and geographically dispersed population, with substantial disparities in access to healthcare services, particularly across underserved rural communities. Geographic isolation, limited healthcare infrastructure, and vulnerability to healthcare-facility closures further contribute to unequal access to care across the state (Hong et al., 2023). These structural and geographic disparities may influence healthcare utilization, diagnostic practices, and antibiotic prescribing patterns, potentially contributing to spatial variation in antimicrobial resistance. If diagnostic or prescribing practices in the state vary systematically with seasonal temperature—for instance, through temperature-linked changes in infection incidence or healthcare-seeking behavior—this could plausibly generate the observed lagged association independently of, or in addition to, a direct thermal effect on bacterial physiology of the kind demonstrated experimentally by Rodríguez-Verdugo et al. (2020). Agricultural and livestock practices, which are not directly measured in this study, offer a further plausible pathway (Usman Qamar and Aatika, 2023). It is emphasized that none of these mechanisms have been tested here; the present study establishes a directional, cross-method-consistent statistical association, not a validated causal pathway, and this is flagged explicitly to avoid overstating what the data support.

5.4 Limitations

Several limitations qualify the interpretation of these findings. First, and most fundamentally, this study's scope has been restricted to climatic (temperature, precipitation) and one socioeconomic (PCPI) driver; it has not included antimicrobial consumption, healthcare access, hospital capacity, diagnostic intensity, infection prevention and control practices, population density, urbanization, or agricultural and livestock antimicrobial use, each of which has been linked to AMR elsewhere in the literature reviewed in Section 2. This is a deliberate scope restriction rather than an oversight, but it means that any of the associations reported here could, in principle, reflect the influence of an unmeasured confounder correlated with both the driver and AMR. PCPI may act as a proxy for healthcare or testing infrastructure rather than, or in addition to, a direct socioeconomic driver of resistance, and this distinction cannot be resolved with the present data. In particular, outpatient antibiotic prescribing varies

substantially across U.S. states, and because antimicrobial use is the principal driver of resistance, this heterogeneity is a major potential confounder that has not been modeled here. Second, the AMR outcome itself is based on the CDC's aggregated "percent resistant" metric (Section 3.2), which, despite the state-level minimum data-availability criteria applied here (Section 3.1), remains subject to variation in testing intensity, laboratory coverage, and reporting practices across states and over time that could not be fully disentangled from genuine epidemiological signal. Third, and most consequentially for statistical power, the underlying AMR series span only fourteen annual observations per phenotype; even after pooling across four phenotypes to partially offset this constraint (Section 3.3), the large majority of nominally significant associations did not survive correction for multiple testing (Section 4.1); moreover, the phenotype-pooling strategy rests on the assumption that the four phenotypes can be treated as independent realizations of a common underlying process, an assumption that could not be directly tested and is unlikely to hold strictly. The four phenotypes share the same state-year climatic and socioeconomic series and the same surveillance system, and they overlap biologically. The phenotype-level series are therefore positively dependent, so the effective sample size is smaller than the pooled count suggests, and the PCMCI and TE p-values, as well as the Fisher-combined CCM p-values (which assume independence), are likely anti-conservative. The agreement of the four phenotypes in West Virginia (Section 4.4) should accordingly not be read as four independent confirmations. Phenotype-specific or leave-one-phenotype-out analyses are a priority for future work. Fourth, CCM library sizes have been correspondingly small given the fourteen-year annual series (maximum library size = 14; Section 4.4); despite this constraint, CCM nonetheless detected a clear, monotonically converging cross-map skill for the West Virginia–maximum temperature association across all four phenotypes (Figure 16), indicating that the method remained informative even with a limited library size. Finally, as with any causal-discovery method applied to observational data, PCMCI, TE, and CCM identify directional, temporally resolved statistical dependence consistent with a causal interpretation under stated assumptions (causal sufficiency, faithfulness, and stationarity); they do not, by themselves, establish intervention-level causal effects, and the associations reported here should accordingly be interpreted as candidate signals warranting further, mechanistically grounded investigation rather than as confirmed causal relationships.

5.5 Implications

Notwithstanding these limitations, the findings offer modest but concrete support for incorporating climatic and socioeconomic monitoring alongside conventional antimicrobial-use surveillance in AMR mitigation planning, consistent with the One Health perspective advocated throughout the literature reviewed in Section 2 (Klümper et al., 2022; Nguyen-Thanh et al., 2024; Huebner et al., 2025). Rather than supporting broad, nationally uniform policy recommendations, the state- and driver-specific nature of the associations identified here—most notably the temperature association in West Virginia

and the minimum-temperature and income associations distributed across a further eleven states (Table 2)—points toward regionally tailored surveillance and intervention strategies, prioritized toward the small set of state–driver associations supported by convergent evidence from multiple independent methods, as a more defensible use of the present results than any claim of a universal climatic or socioeconomic driver of AMR.

6. Conclusion

AMR is poised to become one of the most significant challenges of our future, impacting not only public health but also the global economy. The existing literature makes it clear that the drivers of AMR are incredibly diverse, demanding a truly comprehensive approach. Understanding, predicting, and modeling AMR is a challenging task. Its drivers are numerous and diverse, exhibiting nonlinear and, in some cases, chaotic behavior across different temporal and spatial scales. Therefore, effectively grasping the dynamics of AMR—and identifying directional, temporally resolved associations with its candidate drivers—requires a holistic perspective. Planning the necessary interventions and protective measures is only possible by integrating a wide array of factors. This includes various climate variables and scenarios, climate–environment interactions, agricultural and livestock activities, and the full spectrum of relevant demographic, social, and economic perspectives.

Several eye-opening studies on AMR have illuminated the path forward, highlighting what needs to be done. In their 2023 work, Usman Qamar and Aatika argue that a solution is impossible if we focus solely on human health. They offer compelling examples: rising temperatures cause stress in animals, lowering their resistance to disease. This, in turn, leads to increased antibiotic use and a subsequent rise in drug-resistant bacteria originating from livestock. Furthermore, they point out that soil and water act as vast reservoirs for resistance genes. Climate change, they warn, is effectively opening up pathways for this reservoir to "leak" into human and animal populations, threatening the health of both.

In their 2022 report, Klümper et al. emphasize the critical importance of environmental surveillance. They argue that current monitoring systems are predominantly focused on clinical (human) and livestock settings, largely overlooking the environment. Given the crucial role that water, soil, and waste play in the spread of resistant bacteria, they advocate for establishing an international, standardized monitoring network. Echoing this sentiment, Gao et al. (2024) similarly contend that managing AMR risk in rivers requires moving beyond local measures. They call for the creation of integrated monitoring systems that incorporate global microbiome data. Their work powerfully suggests that rivers should be evaluated not just for their water quality, but for the "resistance load" they carry.

Nguyen-Thanh et al. (2024) argue that simply restricting antibiotics is not enough. They urge policymakers to treat AMR as a multi-sectoral crisis, stressing that the fight against it must also include tackling poverty, protecting the environment, and ensuring good

governance. Similarly, Huebner et al. (2025) emphasize that while AMR is a global problem, solutions must be tailored to regional dynamics, such as local agriculture and healthcare systems. Their work shows AMR moving in a nonlinear cycle—for instance, from livestock back to humans through the environment. They conclude that the disconnect between medicine, veterinary science, and environmental science hinders progress, and call for these sectors to work from a shared system map.

In their comprehensive review, Ljungqvist et al. (2025) note that low income and income imbalance affect AMR. They underline that unregulated antibiotic access increases abuse in low-GDP areas. Insufficient public awareness of antibiotic efficacy leads to inappropriate use, underscoring that patient and provider education considerably alter prescribing behaviors. The report proposes a "One Health" plan that unites human, animal, and environmental health, supported by strong social policies and international collaboration, to combat AMR.

In light of all this information, the drivers of AMR—which are the focus of this study—clearly warrant further investigation. This work has explored observational causal-discovery signals between AMR in four *E. coli* resistance phenotypes and a set of meteorological variables (maximum temperature, minimum temperature, and precipitation) and a socioeconomic factor (per capita personal income, PCPI) across 49 U.S. states, using three complementary causal-discovery methods—PCMCI, Transfer Entropy, and Convergent Cross Mapping—applied to fourteen years (2011–2024) of pooled, phenotype-replicated annual data. At the nominal $p < 0.05$ threshold, each method identified a substantial number of candidate driver–AMR associations (32 for PCMCI, 26 for TE, 9 for CCM), broadly distributed across states and drivers; after Benjamini-Hochberg FDR correction for multiple testing, the number of associations surviving fell sharply for all three methods, underscoring the exploratory nature of causal discovery from short, annual, state-level series and reinforcing the need for cautious interpretation of any single-method result. To address this limitation, cross-method agreement has been used as an additional robustness criterion: thirteen state–driver pairs have been flagged as significant by at least two of the three methods at $p < 0.1$, most frequently involving minimum temperature and PCPI, while a single association—between maximum temperature and AMR in West Virginia—has been independently identified as significant by all three methods and, uniquely among all associations tested, has survived FDR correction within the CCM analysis alone, supported consistently across all four resistance phenotypes. This convergence of independent evidence represents the most robust finding of this study and offers a concrete, testable target for future mechanistic and surveillance-based investigation.

Beyond this headline result, the three methods also diverged informatively in which drivers they most frequently implicated—temperature extremes for PCMCI, precipitation for TE, and PCPI for CCM—suggesting that these complementary approaches, which differ in their underlying assumptions (parametric conditional independence, information-

theoretic transfer, and nonlinear state-space reconstruction, respectively), are sensitive to different aspects of the driver–AMR relationship rather than converging on a single dominant mechanism. Where PCMCI detected robust, FDR-surviving associations, these most often involved a short lag (0–2 years) between the driver and the observed change in AMR, and the majority of all nominally significant PCMCI associations involved a non-zero lag, consistent with a delayed rather than instantaneous relationship between climatic and economic conditions and resistance levels. Taken together, these results indicate that meteorological factors and income level are plausible, but state- and method-specific, correlates of *E. coli* AMR dynamics in the United States, rather than uniform or universally dominant drivers—a more measured conclusion than earlier framings of this work, and one that better reflects the statistical power attainable from fourteen years of annual, state-level surveillance data, even after pooling across resistance phenotypes.

Drawing from this study and the broader literature, several key conclusions about AMR research can be made. First, data availability stands out as a primary obstacle. This issue is rooted in legal and political barriers to data sharing among countries, the relatively short time span of available AMR data (in the present study, fourteen years, and in general roughly the last fifteen), and the low temporal and spatial resolution of this data; even after pooling across four resistance phenotypes to partially offset this constraint, the present analysis found that the great majority of candidate associations did not survive correction for multiple testing, illustrating concretely how acutely statistical power is constrained by short annual surveillance records. Compounding the problem is the difficulty of accessing information from a single platform, as many nations use their own disparate data portals.

Second, as previously highlighted, tackling AMR demands a remarkably comprehensive approach. It must be multisectoral (integrating policy, economics, health, environment, agriculture, livestock, and tourism), multivariate (including meteorological, environmental, demographic, and socioeconomic drivers), and multistakeholder (involving all countries and a wide range of professionals, from politicians, municipalities, and decision-makers to health, environment, climate, water, agriculture, livestock, and tourism professionals). This approach must be built on a foundation of shared data, following the FAIR (Findable, Accessible, Interoperable, and Reusable) principles.

Furthermore, we must account for complex interactions such as cascading or compound effects. The present findings offer direct empirical support for this point: where robust associations have been detected, the driver most often preceded the observed change in AMR by one or more years (typically 0–2 years among the FDR-surviving PCMCI associations) rather than acting contemporaneously, indicating that a change in an environmental or economic factor may influence AMR only after a delay, and that a variable appearing insignificant in isolation could nonetheless interact with others over time to produce a measurable effect. From the perspective of climatic drivers, this means future work must investigate not only mean meteorological variables but also the causal

links between AMR and extreme or compound events such as floods, droughts, and heatwaves (Yeşilköy, 2026a). This requires building multivariate causal networks that explicitly incorporate such time lags, of the kind explored here. Finally, AMR data should be collected and shared not just at the national level but at much finer spatial and temporal scales than the annual, state-level resolution available for the present study.

To conclude, future work must be grounded in the One Health approach. AMR needs to be studied holistically, with the full participation of all stakeholder domains. Data and findings must be shared transparently to enable comprehensive planning that accounts for all influential drivers, both for today and for the future. The present study, by combining three complementary causal-discovery methods and an explicit, cross-method robustness criterion, offers one step toward this goal—identifying a small set of specific, well-supported state–driver associations, most notably the temperature–AMR coupling observed in West Virginia, as priority candidates for the mechanistic and regionally tailored investigation that this literature consistently calls for.

Acknowledgement

This research was supported in part by an appointment to the NRC Research Associateship Program at the National Oceanic and Atmospheric Administration - Global System Laboratory (NOAA-GSL), administered by the Fellowships Office of the National Academies of Sciences, Engineering, and Medicine. The statements, findings, conclusions, and recommendations are those of the author and do not necessarily reflect the views of NOAA or the U.S. Department of Commerce.

Data Availability

E. coli data from Centers for Disease Control and Prevention (CDC): https://arpsp.cdc.gov/profile/antibiotic-resistance?tab=antibiotic-resistance

Meteorological (Tmax, Tmin and Precipitation) Data from NOAA: https://www.ncei.noaa.gov/access/monitoring/climate-at-a-glance/statewide/time-series/

PCPI data from U.S. Bureau of Economic Analysis (BEA): https://www.bea.gov/itable/

References

Al-Khalaifah, H., Rahman, M. H., Al-Surrayai, T., Al-Dhumair, A., & Al-Hasan, M. (2025). A One-Health perspective of antimicrobial resistance (AMR): Human, animals and environmental health. *Life*, *15*(10), 1598.

Alvy, S. C. (2014). How the FDA Can Strengthen Governing Antibiotic Use in Food-Producing Animals. *J. Animal & Envtl. L.*, *6*, 1.

Awasthi, R., Rakholia, V., Agrawal, S., Dhingra, L. S., Nagori, A., Kaur, H., & Sethi, T. (2022). Estimating the impact of health systems factors on antimicrobial resistance in priority pathogens. *Journal of Global Antimicrobial Resistance*, *30*, 133-142.

Baydaroğlu, Ö., & Koçak, K. (2019). Spatiotemporal analysis of wind speed via the Bayesian maximum entropy approach. *Environmental earth sciences*, *78*(1), 17.

Baydaroğlu, Ö., Yeşilköy, S., Dave, A., Linderman, M., & Demir, I. (2024). Modeling Algal Toxin Dynamics and Integrated Web Framework for Lakes. *Toxins* 2025, *17*(7), 338

Baydaroğlu, Ö. (2025). Harmful algal bloom prediction using empirical dynamic modeling. *Science of The Total Environment*, *959*, 178185.

Bartsev, S., Saltykov, M., Belolipetsky, P., & Pianykh, A. (2021, February). Imperfection of the convergent cross-mapping method. *In IOP Conference Series: Materials Science and Engineering* (Vol. 1047, No. 1, p. 012081). IOP Publishing.

Benjamini, Y., & Hochberg, Y. (1995). Controlling the false discovery rate: a practical and powerful approach to multiple testing. *Journal of the Royal statistical society: series B (Methodological)*, *57*(1), 289-300.

Bonotto, G., Peterson, T. J., Fowler, K., & Western, A. W. (2022). Identifying causal interactions between groundwater and streamflow using convergent cross-mapping. *Water Resources Research*, 58(8), e2021WR030231.

Booth, A., & Wester, A. L. (2022). A multivariable analysis of the contribution of socioeconomic and environmental factors to blood culture Escherichia coli resistant to fluoroquinolones in high-and middle-income countries. *BMC Public Health*, *22*(1), 354.

Centers for Disease Control and Prevention. (2022). *COVID-19: U.S. impact on antimicrobial resistance, special report 2022*. U.S. Department of Health and Human Services. https://www.cdc.gov/drugresistance/covid19.html

Chayña, E. T., Ferro, P., Morales-Rojas, E., Ferro-Gonzales, A. L., Nuñez, J. B., Pedraza, E. V., ... & Ferro-Gonzales, P. (2025). Detection of Antibiotic-Resistance Genes in Drinking Water: A Study at a University in the Peruvian Amazon. *International Journal of Environmental Research and Public Health*, *22*(3), 353.

Ching, C., Sutradhar, I., & Zaman, M. H. (2025). Understanding the impacts of temperature and precipitation on antimicrobial resistance in wastewater: theory, modeling, observation, and limitations. *mSphere*, *10*(3), e00947-24.

Collignon, P., Athukorala, P. C., Senanayake, S., & Khan, F. (2015). Antimicrobial resistance: the major contribution of poor governance and corruption to this growing problem. *PloS one*, *10*(3), e0116746.

Csorba, S., Vribék, K., Farkas, M., Süth, M., Strang, O., Zentai, A., & Farkas, Z. (2025). Data-Driven Early Warning Approach for Antimicrobial Resistance Prediction–Anomaly Detection Based on High-Level Indicators. *Veterinary Sciences*, *12*(10), 935.

Dadgostar, P. (2019). Antimicrobial resistance: implications and costs. *Infection and drug resistance*, 3903-3910.

Deb, L. C., Jara, M., & Lanzas, C. (2023). Early evaluation of the Food and Drug Administration (FDA) guidance on antimicrobial use in food animals on antimicrobial resistance trends reported by the National Antimicrobial Resistance Monitoring System (2012–2019). *One Health*, *17*, 100580.

Delforge, D., de Viron, O., Vanclooster, M., Van Camp, M., & Watlet, A. (2022). Detecting hydrological connectivity using causal inference from time series: synthetic and real karstic case studies. *Hydrology and Earth System Sciences*, *26*(8), 2181-2199.

Díaz-Zaragoza, M., Rodriguez-Preciado, S. Y., Hernández-Ventura, L., Ortiz-Covarrubias, A., Castellanos-García, G., Sifuentes-Franco, S., ... & Macias-Barragan, J. (2025). Evaluation of Antibiotic Resistance in Escherichia coli Isolated from a Watershed Section of Ameca River in Mexico. *Microbiology Research*, *16*(8), 186.

Docquier, D., Di Capua, G., Donner, R. V., Pires, C. A., Simon, A., & Vannitsem, S. (2024). A comparison of two causal methods in the context of climate analyses. *Nonlinear Processes in Geophysics*, *31*(1), 115-136.

Donaghy, J. A., Jagadeesan, B., Goodburn, K., Grunwald, L., Jensen, O. N., Jespers, A. D., ... & Quentin, M. C. (2019). Relationship of sanitizers, disinfectants, and cleaning agents with antimicrobial resistance. *Journal of Food Protection*, *82*(5), 889-902.

Fisher, R. A. (1932). Statistical methods for research workers. (4th ed.). Oliver & Boyd.

Gao, F. Z., He, L. Y., Liu, Y. S., Zhao, J. L., Zhang, T., & Ying, G. G. (2024). Integrating global microbiome data into antibiotic resistance assessment in large rivers. *Water research*, *250*, 121030.

Graham, D. W., Bergeron, G., Bourassa, M. W., Dickson, J., Gomes, F., Howe, A., ... & Wittum, T. E. (2019). Complexities in understanding antimicrobial resistance across domesticated animal, human, and environmental systems. *Annals of the New York Academy of Sciences*, *1441*(1), 17-30.

Granger, C. W. (1969). Investigating causal relations by econometric models and cross-spectral methods. *Econometrica: journal of the Econometric Society*, 424-438.

Hong, I., Wilson, B., Gross, T., Conley, J., & Powers, T. (2023). Challenging terrains: socio-spatial analysis of primary health care access disparities in West Virginia. *Applied spatial analysis and policy*, *16*(1), 141-161.

Huebner, C., Huebner, N. O., Goerig, T., & Flessa, S. (2025). A regional One Health approach to mapping antimicrobial resistance interactions via systems thinking. *One Health Outlook*, *7*(1), 46.

Iacobucci, G. (2024). Fluoroquinolone antibiotics: Prescribe only as last resort, says UK regulator. *BMJ: British Medical Journal (Online)*, *384*, q183.

Kalanxhi, E., & Laxminarayan, R. (2026). Climate change and antimicrobial resistance. *Nature Reviews Microbiology*, 1-12.

Kardish, M. R., Agans, R. T., Barbato, R. A., Doherty, S. J., Goodson, M. S., Karl, J. P., ... & Leary, D. H. (2025, December). Meeting report of the eight annual Tri-Service Microbiome Consortium Symposium. In *BMC proceedings* (Vol. 20, No. Suppl 2, p. 2). London: BioMed Central.

Kirby, A., & Herbert, A. (2013). Correlations between income inequality and antimicrobial resistance. *PLoS One*, *8*(8), e73115.

Klümper, U., Leonard, A. F. C., Stanton, I. C., Ajun, M. F., Antonio, M., & Balkhy, H. (2022). Towards developing an international environmental AMR surveillance strategy. *JPIAMR Rep*.

Kou, R., Wang, H., Zou, D., Hu, J., Wu, Y., Xu, Q., & Zhang, X. (2025). Spatial panel data analysis of antimicrobial resistance in Escherichia coli in China. *Scientific Reports*, *15*(1), 23753.

Krich, C., Runge, J., Miralles, D. G., Migliavacca, M., Perez-Priego, O., El-Madany, T., ... & Mahecha, M. D. (2020). Estimating causal networks in biosphere–atmosphere interaction with the PCMCI approach. *Biogeosciences*, *17*(4), 1033-1061.

Kullback, S. (1951). Kullback-leibler divergence.

Leekitcharoenphon, P., Johansson, M. H. K., Munk, P., Malorny, B., Skarżyńska, M., Wadepohl, K., ... & Aarestrup, F. M. (2021). Genomic evolution of antimicrobial resistance in Escherichia coli. *Scientific reports*, *11*(1), 15108.

Li, W., Huang, T., Liu, C., Wushouer, H., Yang, X., Wang, R., ... & Yang, L. (2025). Changing climate and socioeconomic factors contribute to global antimicrobial resistance. *Nature Medicine*, *31*(6), 1798-1808.

Ljungqvist, G., van Kessel, R., Mossialos, E., Saint, V., Schmidt, J., Mafi, A., ... & Anderson, M. (2025). Mapping socioeconomic factors driving antimicrobial resistance in humans: An umbrella review. *One Health*, *20*, 100986.

MacFadden, D. R., McGough, S. F., Fisman, D., Santillana, M., & Brownstein, J. S. (2018). Antibiotic resistance increases with local temperature. *Nature Climate Change*, *8*(6), 510-514.

MacKinnon, M. C., Sargeant, J. M., Pearl, D. L., Reid-Smith, R. J., Carson, C. A., Parmley, E. J., & McEwen, S. A. (2020). Evaluation of the health and healthcare system burden due to antimicrobial-resistant Escherichia coli infections in humans: a systematic review and meta-analysis. *Antimicrobial Resistance & Infection Control*, *9*(1), 200.

Martínez, E. P., Verbon, A., Schoffelen, A. F., Altorf-van der Kuil, W., van Rosmalen, J., Stuart, J. W. C., ... & Machiels, J. D. (2025). Dynamic association of antimicrobial resistance in urinary isolates of Escherichia coli and Klebsiella pneumoniae between primary care and hospital settings in the Netherlands (2008–2020): a population-based study. *The Lancet Regional Health–Europe*, *50*.

Meinen, A., Tomczyk, S., Wiegand, F. N., Sin, M. A., Eckmanns, T., & Haller, S. (2023). Antimicrobial resistance in Germany and Europe–A systematic review on the increasing threat accelerated by climate change. *Journal of Health Monitoring*, *8*(Suppl 3), 93.

Matijašević, D., Kljajević, N., Malešević, M., Gardijan, L., Stanovčić, S., Jovčić, B., & Novović, K. (2026). Heating-season dynamics of the airborne microbiome, resistome and mobilome in Belgrade, Serbia. *Environment International*, 110114.

Moncada Muñoz, P. M. (2019). *Antimicrobial resistance in Honduran salmonella and in Escherichia coli recovered from cattle in the US* (Doctoral dissertation).

Moon, K., van Bavel, B., Berrang Ford, L., Badger, K., Carter, L., Evans, B., ... & King, R. (2025). A research agenda advancing climate change and antimicrobial resistance as interconnected issues. *Nature Climate Change*, 1-4.

Murray, C. J., Ikuta, K. S., Sharara, F., Swetschinski, L., Aguilar, G. R., Gray, A., ... & Tasak, N. (2022). Global burden of bacterial antimicrobial resistance in 2019: a systematic analysis. *The lancet*, *399*(10325), 629-655.

Muszynski, G., Orr, A., Roy, I., Di Capua, G., Pritchard, H. D., & Scott Hosking, J. (2026). Using a causal effect network approach to quantify the impact of ENSO teleconnections on summer monsoon precipitation over the Himalayas and key regional circulations. *Quarterly Journal of the Royal Meteorological Society*, e70114.

Naghavi, M., Vollset, S. E., Ikuta, K. S., Swetschinski, L. R., Gray, A. P., Wool, E. E., ... & Dekker, D. M. (2024). Global burden of bacterial antimicrobial resistance 1990–2021: a systematic analysis with forecasts to 2050. *The Lancet*, *404*(10459), 1199-1226.

Nguyen-Thanh, L., Wernli, D., Målqvist, M., Graells, T., & Jørgensen, P. S. (2024). Characterising proximal and distal drivers of antimicrobial resistance: An umbrella review. *Journal of Global Antimicrobial Resistance*, *36*, 50-58.

Özbek, M. (2026). Antimicrobial resistance and environmental–lifestyle exposures: A canonical analysis of national mortality indicators. *Science of The Total Environment*, *1012*, 181273.

Papp-Wallace, K. M., Endimiani, A., Taracila, M. A., & Bonomo, R. A. (2011). Carbapenems: past, present, and future. *Antimicrobial agents and chemotherapy*, *55*(11), 4943-4960.

Paterson, D. L. (2000). Recommendation for treatment of severe infections caused by Enterobacteriaceae producing extended-spectrum β-lactamases (ESBLs). *Clinical Microbiology and Infection*, *6*(9), 460-463.

Rodríguez-Verdugo, A., Lozano-Huntelman, N., Cruz-Loya, M., Savage, V., & Yeh, P. (2020). Compounding effects of climate warming and antibiotic resistance. *IScience*, *23*(4).

Ruiz-Perez, D., Gimon, I., Sazal, M., Mathee, K., & Narasimhan, G. (2024). Unfolding and de-confounding: biologically meaningful causal inference from longitudinal multi-omic networks using METALICA. *Msystems*, *9*(10), e01303-23.

Runge, J., Petoukhov, V., Donges, J. F., Hlinka, J., Jajcay, N., Vejmelka, M., ... & Kurths, J. (2015). Identifying causal gateways and mediators in complex spatio-temporal systems. *Nature communications*, *6*(1), 8502.

Runge, J., Bathiany, S., Bollt, E., Camps-Valls, G., Coumou, D., Deyle, E., ... & Zscheischler, J. (2019). Inferring causation from time series in Earth system sciences. *Nature communications*, *10*(1), 2553.

Runge, J., Nowack, P., Kretschmer, M., Flaxman, S., & Sejdinovic, D. (2019). Detecting and quantifying causal associations in large nonlinear time series datasets. *Science advances*, *5*(11), eaau4996.

Schreiber, T. (2000). Measuring information transfer. *Physical review letters*, *85*(2), 461.

Shannon, C. E. (1948). A mathematical theory of communication. *The Bell system technical journal*, *27*(3), 379-423.

Sironen, A. (2020). Transfer Entropy and Applications to Ecosystem Atmospheric Data.

Spirtes, P., & Glymour, C. (1991). An algorithm for fast recovery of sparse causal graphs. *Social science computer review*, *9*(1), 62-72.

Spirtes, P., Glymour, C., & Scheines, R. (2000). Causation, Prediction, and Search. Adaptive Computation and Machine Learning Series. *The MIT Press*, *49*, 77-78.

Sugihara, G., May, R., Ye, H., Hsieh, C. H., Deyle, E., Fogarty, M., & Munch, S. (2012). Detecting causality in complex ecosystems. *science*, *338*(6106), 496-500.

Sutradhar, I., Ching, C., Desai, D., Suprenant, M., Briars, E., Heins, Z., ... & Zaman, M. H. (2021). Computational model to quantify the growth of antibiotic-resistant bacteria in wastewater. *Msystems*, *6*(3), 10-1128.

Takens, F., 1981. Detecting strange attractors in turbulence. In: Rand, D.A, Young, L.S. (Eds.), Lecture Notes in Math. Springer-Verlag, pp. 366–381.

Torres, J. A., Villegas, M. V., & Quinn, J. P. (2007). Current concepts in antibiotic-resistant gram-negative bacteria. *Expert review of anti-infective therapy*, *5*(5), 833-843.

United Nations General Assembly. (2024). Political declaration of the high-level meeting on antimicrobial resistance.

U.S. Food and Drug Administration. (2012). *Guidance for industry #209: The judicious use of medically important antimicrobial drugs in food-producing animals*. U.S. Department of Health and Human Services. https://www.fda.gov/regulatory-information/search-fda-guidance-documents/cvm-gfi-209-judicious-use-medically-important-antimicrobial-drugs-food-producing-animals

US Department of Health and Human Services. (2019). *CDC. Antibiotic Resistance Threats in the United States, 2019. Atlanta, GA*.

Shannon, C. E. (1948). A mathematical theory of communication. *The Bell system technical journal*, *27*(3), 379-423.

Usman Qamar, M., & Aatika. (2023). Impact of climate change on antimicrobial resistance dynamics: an emerging One Health challenge. *Future Microbiology*, *18*(9), 535-539.

Vicente, R., Wibral, M., Lindner, M., & Pipa, G. (2011). Transfer entropy—a model-free measure of effective connectivity for the neurosciences. Journal of computational neuroscience, 30(1), 45-67.

Wang, Y., Xu, X., Jia, S., Qu, M., Pei, Y., Qiu, S., ... & Gao, G. F. (2025). A global atlas and drivers of antimicrobial resistance in Salmonella during 1900-2023. *Nature Communications*, *16*(1), 4611.

Woolhouse, M., Ward, M., Van Bunnik, B., & Farrar, J. (2015). Antimicrobial resistance in humans, livestock and the wider environment. *Philosophical Transactions of the Royal Society B: Biological Sciences*, *370*(1670), 20140083.

Yang, L., Ma, Z., Meng, F., Wang, R., Chen, S., Liu, C., ... & Ji, J. S. (2026). Climate change and antimicrobial resistance in the Western Pacific: a mixed-methods systematic analysis. *The Lancet Regional Health–Western Pacific*, *67*.

Yazdankhah, S., Skjerve, E., & Wasteson, Y. (2018). Antimicrobial resistance due to the content of potentially toxic metals in soil and fertilizing products. *Microbial ecology in health and disease*, *29*(1), 1548248.

Yeşilköy, S., Baydaroğlu, Ö. & Demir, I (2026). Linking drought indicators and crop yields through causality and information transfer: a phenology-based analysis. Sci Rep 16, 2373.

Yeşilköy, S. (2026a). Quantifying the Causal Strength of Compound Drought–Heatwaves: Implications for Fire Events and Cropland Productivity. Eartharxiv DOI: https://doi.org/10.31223/X5BX8V

Yeşilköy, S. (2026b). Heatwave Characteristics in Agricultural and Forest Lands across Türkiye: Historical and Future Insights from CMIP6 Simulations. *International Journal of Environment and Geoinformatics*, *12*(4), 440-451.

Zeng, Y., Li, W., Zhao, M., Li, J., Liu, X., Shi, L., ... & Yang, L. (2023). The association between ambient temperature and antimicrobial resistance of Klebsiella pneumoniae in China: a difference-in-differences analysis. Frontiers in Public Health, 11, 1158762.

Zambrano, M. M. (2023). Interplay between antimicrobial resistance and global environmental change. *Annual Review of Genetics*, *57*(1), 275-296.

Zhao, W., Wu, J., Jiang, X., He, T., & Hu, X. (2024). Causal-ARG: a causality-guided framework for annotating properties of antibiotic resistance genes. *Bioinformatics*, *40*(4), btae180.

Zhou, X. Y., Hu, A., Huang, F. Y., Jensen, M. K. S., Zhao, Y., Yan, X. P., ... & Su, J. Q. (2024). Reduction in antimicrobial resistance in a watershed after closure of livestock farms. Environment International, 190, 108846.

URL-1: https://www.fda.gov/drugs/drug-safety-and-availability/fda-drug-safety-communication-fda-advises-restricting-fluoroquinolone-antibiotic-use-certain#:~:text= The%20FDA%20recommends%20that%20fluoroquinolones%20be%20reserved,or%20pricking%20sensation%20%20Confusion%20*%20Hallucinations*

6. Appendix

Table S1. State-level phenotype data availability and pooled sample size used in the causal-discovery analyses (PCMCI, CCM, and TE).

Resistance data for four E. coli phenotypes (multidrug-resistant [MDR], carbapenem-resistant, cephalosporin-resistant, and fluoroquinolone-resistant) have been pooled as independent annual realizations for each state, subject to a minimum data-availability requirement per phenotype. For most states with n < 56, the sole source of missing observations was the unavailability of 2011 data (the first year of the CDC Antibiotic Resistance surveillance program) across all phenotypes, reducing the available record to 13 years. Rows shaded in orange indicate the three states for which carbapenem-resistant E. coli data availability fell below that of other states and was therefore excluded from pooling for that phenotype.

State	Phenotypes Pooled (of 4)	Excluded Phenotype(s)	Pooled n	Notes on Missing Annual Observations
Alabama	4/4	None	56	—
Alaska	3/4	*Carbapenem*	39	MDR missing [2011]; Cephalosporin missing [2011]; Fluoroquinolone missing [2011]
Arizona	4/4	None	56	—
Arkansas	4/4	None	56	—
California	4/4	None	56	—
Colorado	4/4	None	56	—

State	Phenotypes Pooled (of 4)	Excluded Phenotype(s)	Pooled n	Notes on Missing Annual Observations
Connecticut	4/4	None	52	2011 not available for any phenotype (state did not yet report to CDC AR surveillance in the program's first year)
Delaware	3/4	*Carbapenem*	42	—
Florida	4/4	None	56	—
Georgia	4/4	None	56	—
Hawaii	4/4	None	56	—
Idaho	4/4	None	52	2011 not available for any phenotype (state did not yet report to CDC AR surveillance in the program's first year)
Illinois	4/4	None	56	—
Indiana	4/4	None	56	—
Iowa	4/4	None	56	—
Kansas	4/4	None	56	—
Kentucky	4/4	None	56	—
Louisiana	4/4	None	56	—
Maine	4/4	None	56	—
Maryland	4/4	None	56	—
Massachusetts	4/4	None	56	—
Michigan	4/4	None	56	—
Minnesota	4/4	None	56	—
Mississippi	4/4	None	56	—
Missouri	4/4	None	55	Carbapenem missing [2011]
Montana	4/4	None	56	—
Nebraska	4/4	None	56	—
Nevada	4/4	None	56	—
New Hampshire	4/4	None	52	2011 not available for any phenotype (state did not yet report to CDC AR surveillance in the program's first year)
New Jersey	4/4	None	56	—

State	Phenotypes Pooled (of 4)	Excluded Phenotype(s)	Pooled n	Notes on Missing Annual Observations
New Mexico	4/4	None	52	2011 not available for any phenotype (state did not yet report to CDC AR surveillance in the program's first year)
New York	4/4	None	56	—
North Carolina	4/4	None	56	—
North Dakota	3/4	*Carbapenem*	31	MDR missing [2011, 2014, 2023]; Cephalosporin missing [2011, 2012, 2013, 2014, 2023]; Fluoroquinolone missing [2011, 2014, 2023]
Ohio	4/4	None	56	—
Oklahoma	4/4	None	56	—
Oregon	4/4	None	56	—
Pennsylvania	4/4	None	56	—
Rhode Island	4/4	None	56	—
South Carolina	4/4	None	56	—
South Dakota	4/4	None	52	2011 not available for any phenotype (state did not yet report to CDC AR surveillance in the program's first year)
Tennessee	4/4	None	56	—
Texas	4/4	None	56	—
Utah	4/4	None	52	2011 not available for any phenotype (state did not yet report to CDC AR surveillance in the program's first year)
Vermont	4/4	None	51	MDR missing [2011]; Carbapenem missing [2011]; Cephalosporin missing [2011, 2013]; Fluoroquinolone missing [2011]
Virginia	4/4	None	56	—
Washington	4/4	None	56	—
West Virginia	4/4	None	56	—
Wisconsin	4/4	None	56	—

Note: Washington, D.C. and Wyoming are not included in this table, as neither jurisdiction had AMR surveillance records for any phenotype and were excluded from the study entirely (see Section 3.1). States not listed in the Notes column had complete 2011–2024 records for all pooled phenotypes (n = 56).

CCM Diagnostic Plots

This section presents a representative selection of the diagnostic plots underlying the CCM analysis (Section 4.4): simplex projection and S-map nonlinearity tests for the four phenotypes contributing to the study's strongest finding (West Virginia maximum temperature), together with two contrasting examples—a phenotype excluded from CCM due to confirmed linearity and a non-significant, non-convergent association—illustrating that the CCM-eligibility and significance criteria applied throughout this study are not uniformly favorable. The complete set of diagnostic plots for all 196 state–driver combinations (n = 1,055 figures) is available from the corresponding author upon request.

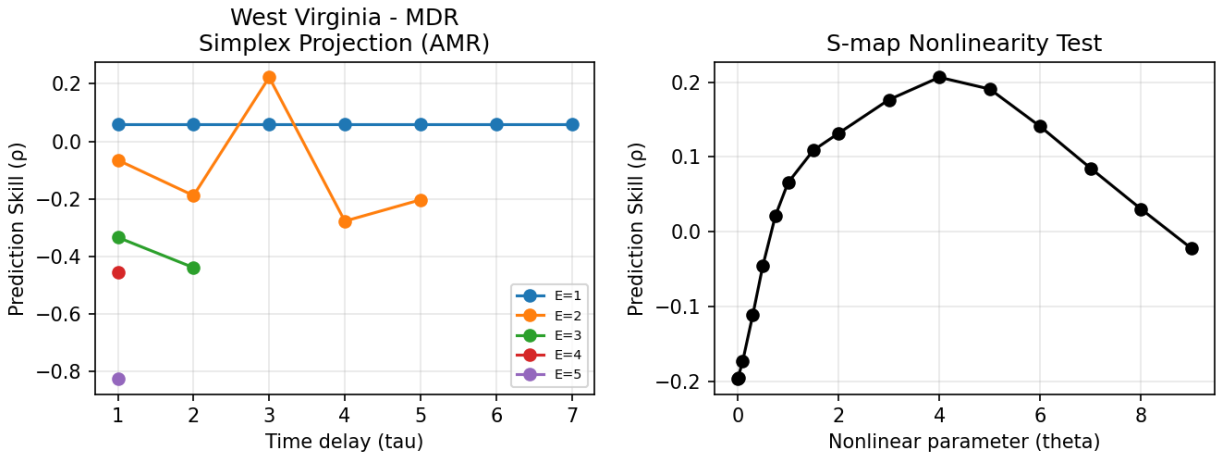


Figure S1. Simplex projection (embedding selection) and S-map nonlinearity test for MDR-resistant E. coli AMR in West Virginia. The S-map prediction skill is maximized at a nonlinear parameter (theta) greater than zero, confirming nonlinear dynamics and CCM eligibility.

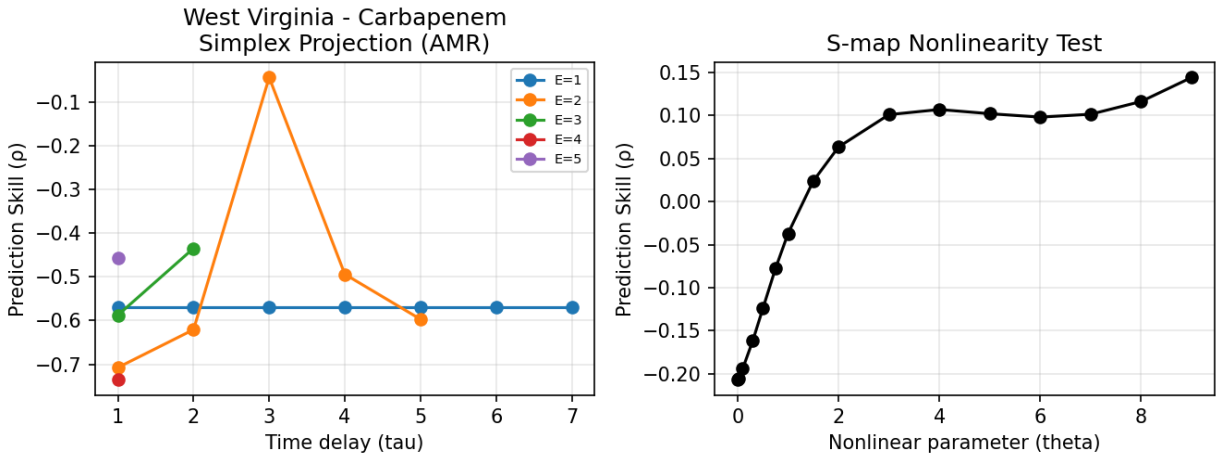


Figure S2. Simplex projection (embedding selection) and S-map nonlinearity test for carbapenem-resistant E. coli AMR in West Virginia.

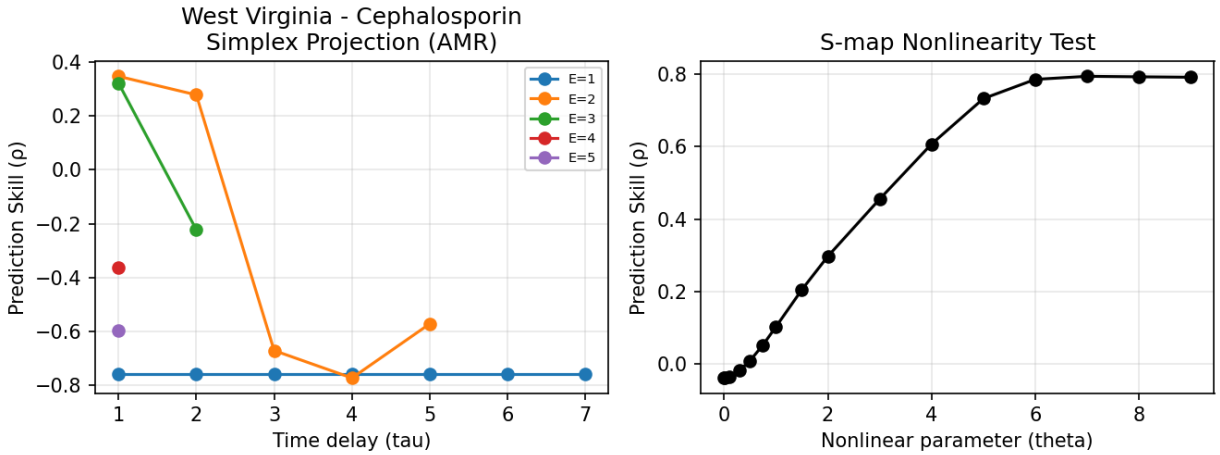


Figure S3. Simplex projection (embedding selection) and S-map nonlinearity test for cephalosporin-resistant E. coli AMR in West Virginia.

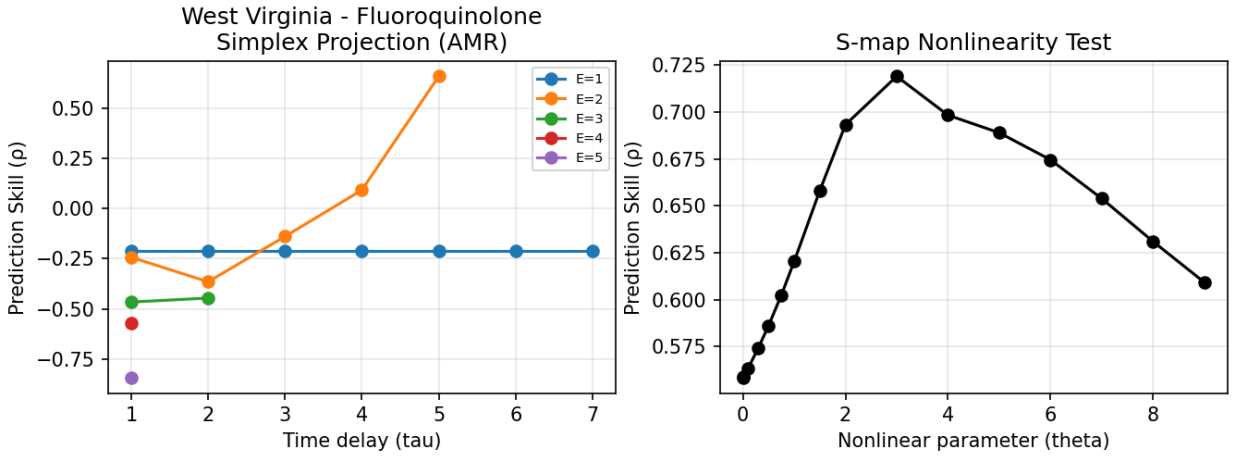


Figure S4. Simplex projection (embedding selection) and S-map nonlinearity test, for fluoroquinolone-resistant E. coli AMR in West Virginia.

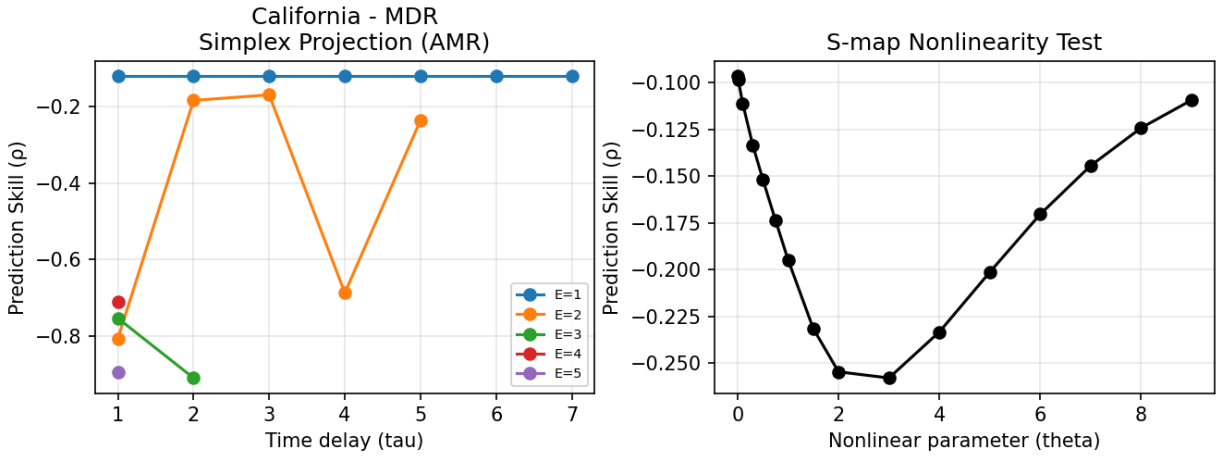


Figure S5. Representative example of a phenotype excluded from CCM testing due to confirmed linearity: MDR-resistant E. coli AMR in California. The S-map prediction skill is maximized at a nonlinear parameter (theta) of zero, indicating linear dynamics; this phenotype was therefore not CCM-eligible for California and was excluded from the Fisher combination for all four drivers in this state, illustrating that the nonlinearity criterion described in Section 3.3.3 is applied selectively rather than uniformly.

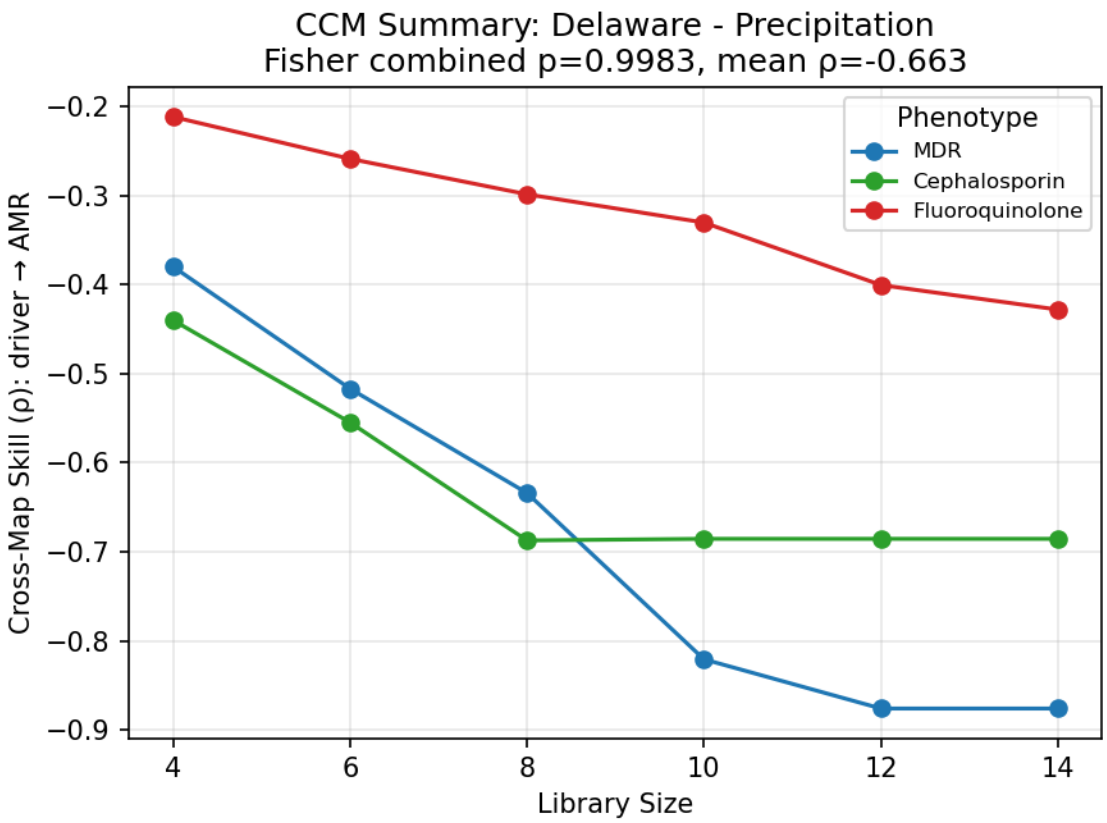


Figure S6. Representative example of a non-significant, non-convergent CCM association: Delaware–precipitation (Fisher-combined p = 0.998; mean ρ = −0.663). In contrast to the West Virginia–maximum temperature association (Figure 16), cross-map skill decreases or plateaus with increasing library size for all three CCM-eligible phenotypes, consistent with the absence of CCM convergence..

Table S2. Full state–driver results across all three causal-discovery methods and descriptive Pearson correlation, at the nominal $p < 0.05$ threshold. Note on sign interpretation: PCMCI and Corr (Pearson correlation) values are directional (positive = positive association, negative = inverse association). TE values are non-negative by construction (Section 3.3.2) and reflect the magnitude of information transfer only, not its direction. CCM values (ρ) reflect cross-map prediction skill; while ρ can range from −1 to 1, its sign should not be interpreted as a directional coefficient in the same sense as PCMCI or Corr. Accordingly, apparent differences in sign between TE or CCM and PCMCI/Corr for the same driver–state pair do not represent a contradiction.

Drivers	PCPI				Precipitation				Maximum Temperature				Minimum Temperature			
Methods States	PCMCI	TE	CCM	Corr	PCMCI	TE	CCM	Corr	PCMCI	TE	CCM	Corr	PCMCI	TE	CCM	Corr
Alabama	x	0.409	x	x	x	x	x	x	0.529	x	x	x	x	x	x	x
Alaska	x	x	0.096	-0.322	x	0.417	x	x	x	x	x	x	x	x	x	x
Arizona	x	x	x	0.296	x	x	x	x	x	x	x	x	x	x	x	x
Arkansas	x	x	x	x	x	x	x	0.482	x	x	0.047	x	x	x	x	x
California	x	x	x	x	x	x	x	x	x	x	x	x	x	x	x	x
Colorado	x	x	x	0.28	x	x	x	0.326	0.652	x	x	x	-0.464	x	x	x
Connecticut	0.515	x	x	x	x	x	x	x	x	x	x	x	x	0.296	x	x
Delaware	x	x	x	x	x	x	x	x	x	x	x	x	x	x	x	x
Florida	-0.549	x	x	x	x	0.272	x	x	x	x	x	x	x	x	x	x
Georgia	x	x	x	0.43	x	x	x	x	x	x	x	x	x	x	x	x
Hawaii	x	x	x	x	0.572	x	x	x	x	x	x	x	0.583	0.323	x	-0.326
Idaho	x	x	x	x	x	x	x	x	x	x	x	x	x	x	x	x
Illinois	x	x	x	x	x	x	x	x	0.875	x	x	x	x	x	x	x
Indiana	x	x	x	x	x	x	x	x	x	x	x	0.412	-0.666	x	x	x
Iowa	-0.705	x	x	x	0.627	x	x	x	x	x	x	x	-0.681	x	x	x
Kansas	0.527	x	x	x	0.606	x	x	x	x	0.376	x	x	0.459	0.406	x	x
Kentucky	x	x	x	-0.294	x	x	x	-0.38	x	x	x	x	x	x	x	x
Louisiana	x	x	x	x	x	0.241	x	x	0.646	x	x	x	x	x	x	x
Maine	x	x	x	x	x	x	x	x	x	x	x	x	0.633	x	x	x
Maryland	x	x	x	x	x	x	x	x	x	x	x	x	-0.674	x	x	x
Massachusetts	x	x	x	x	x	0.344	x	x	x	x	x	x	x	x	x	x
Michigan	x	x	x	x	x	x	x	x	x	x	x	x	x	0.265	x	x
Minnesota	x	x	x	-0.319	x	0.321	x	x	x	0.301	x	x	x	x	x	x
Mississippi	x	x	0.011	x	x	x	x	x	x	x	x	x	x	x	x	x
Missouri	x	x	x	x	x	x	x	x	x	x	x	x	x	x	x	x
Montana	x	x	x	x	x	x	x	x	x	x	x	x	x	0.291	x	x
Nebraska	x	x	x	x	x	0.212	x	x	-0.593	x	x	x	-0.647	0.181	x	x
Nevada	x	x	x	x	x	x	x	x	x	x	x	x	x	x	x	x
New Hampshire	-0.513	x	x	x	x	x	x	x	x	x	x	x	0.51	x	x	x
New Jersey	x	x	x	x	x	x	x	-0.303	x	x	x	x	x	x	x	x
New Mexico	x	x	x	x	x	x	x	x	x	x	x	x	0.591	x	x	x
New York	0.593	x	0.368	x	x	0.248	x	x	x	x	x	x	x	x	x	x
North Carolina	x	x	x	x	x	0.204	x	-0.346	x	x	x	x	x	x	x	x
North Dakota	x	x	x	x	x	x	x	x	x	x	x	x	x	x	x	x
Ohio	x	0.365	x	x	x	x	x	x	0.627	x	x	x	x	x	x	x
Oklahoma	x	0.31	x	x	x	x	x	-0.36	x	x	x	x	x	x	x	-0.281
Oregon	x	x	0.374	-0.382	x	x	x	x	x	x	x	-0.275	x	x	0.158	-0.353
Pennsylvania	x	x	x	x	x	x	x	x	x	x	x	x	x	x	x	x
Rhode Island	x	x	0.255	x	x	x	x	x	x	x	x	x	x	x	x	x
South Carolina	x	x	x	x	x	x	x	x	x	x	x	x	x	x	x	x
South Dakota	x	x	x	x	-0.8	x	x	x	-0.652	x	x	x	0.73	x	x	x
Tennessee	x	x	x	x	x	x	x	x	-0.515	x	x	x	x	x	x	x
Texas	x	x	x	x	x	x	x	x	x	x	x	x	x	x	x	x
Utah	x	x	x	x	x	x	x	-0.339	x	0.237	x	0.293	-0.717	x	x	x
Vermont	0.718	x	x	x	x	x	x	x	0.962	x	x	x	x	x	x	x
Virginia	x	x	x	x	x	x	x	x	x	x	x	x	x	x	x	x
Washington	x	0.321	x	x	x	x	x	x	x	x	x	x	x	x	x	x
West Virginia	x	0.379	x	0.333	x	0.336	x	x	x	0.379	0.509	0.363	x	0.377	x	x
Wisconsin	x	x	0.212	x	x	0.294	x	0.326	x	x	x	x	x	x	x	x

Table S3. Full state–driver results across all three causal-discovery methods and descriptive Pearson correlation, restricted to associations surviving FDR correction at $p < 0.05$. Note on sign interpretation: PCMCI and Corr (Pearson correlation) values are directional (positive = positive association, negative = inverse association). TE values are non-negative by construction (Section 3.3.2) and reflect the magnitude of information transfer only, not its direction. CCM values (ρ) reflect cross-map prediction skill; while ρ can range from −1 to 1, its sign should not be interpreted as a directional coefficient in the same sense as PCMCI or Corr. Accordingly, apparent differences in sign between TE or CCM and PCMCI/Corr for the same driver–state pair do not represent a contradiction.

	PCPI				Precipitation				Maximum Temperature				Minimum Temperature			
Methods States	PCMCI	TE	CCM	Corr	PCMCI	TE	CCM	Corr	PCMCI	TE	CCM	Corr	PCMCI	TE	CCM	Corr
Alabama	x	x	x	x	x	x	x	x	x	x	x	x	x	x	x	x
Alaska	x	x	x	x	x	x	x	x	x	x	x	x	x	x	x	x
Arizona	x	x	x	x	x	x	x	x	x	x	x	x	x	x	x	x
Arkansas	x	x	x	x	x	x	x	0.482	x	x	x	x	x	x	x	x
California	x	x	x	x	x	x	x	x	x	x	x	x	x	x	x	x
Colorado	x	x	x	x	x	x	x	x	0.652	x	x	x	x	x	x	x
Connecticut	x	x	x	x	x	x	x	x	x	x	x	x	x	x	x	x
Delaware	x	x	x	x	x	x	x	x	x	x	x	x	x	x	x	x
Florida	x	x	x	x	x	x	x	x	x	x	x	x	x	x	x	x
Georgia	x	x	x	x	x	x	x	x	x	x	x	x	x	x	x	x
Hawaii	x	x	x	x	x	x	x	x	x	x	x	x	x	x	x	x
Idaho	x	x	x	x	x	x	x	x	x	x	x	x	x	x	x	x
Illinois	x	x	x	x	x	x	x	x	0.875	x	x	x	x	x	x	x
Indiana	x	x	x	x	x	x	x	x	x	x	x	x	x	x	x	x
Iowa	x	x	x	x	x	x	x	x	x	x	x	x	x	x	x	x
Kansas	x	x	x	x	x	x	x	x	x	x	x	x	x	x	x	x
Kentucky	x	x	x	x	x	x	x	x	x	x	x	x	x	x	x	x
Louisiana	x	x	x	x	x	x	x	x	x	x	x	x	x	x	x	x
Maine	x	x	x	x	x	x	x	x	x	x	x	x	x	x	x	x
Maryland	x	x	x	x	x	x	x	x	x	x	x	x	x	x	x	x
Massachusetts	x	x	x	x	x	x	x	x	x	x	x	x	x	x	x	x
Michigan	x	x	x	x	x	x	x	x	x	x	x	x	x	x	x	x
Minnesota	x	x	x	x	x	x	x	x	x	x	x	x	x	x	x	x
Mississippi	x	x	x	x	x	x	x	x	x	x	x	x	x	x	x	x
Missouri	x	x	x	x	x	x	x	x	x	x	x	x	x	x	x	x
Montana	x	x	x	x	x	x	x	x	x	x	x	x	x	x	x	x
Nebraska	x	x	x	x	x	x	x	x	x	x	x	x	-0.647	x	x	x
Nevada	x	x	x	x	x	x	x	x	x	x	x	x	x	x	x	x
New Hampshire	x	x	x	x	x	x	x	x	x	x	x	x	x	x	x	x
New Jersey	x	x	x	x	x	x	x	x	x	x	x	x	x	x	x	x
New Mexico	x	x	x	x	x	x	x	x	x	x	x	x	x	x	x	x
New York	x	x	x	x	x	x	x	x	x	x	x	x	x	x	x	x
North Carolina	x	x	x	x	x	x	x	x	x	x	x	x	x	x	x	x
North Dakota	x	x	x	x	x	x	x	x	x	x	x	x	x	x	x	x
Ohio	x	x	x	x	x	x	x	x	x	x	x	x	x	x	x	x
Oklahoma	x	x	x	x	x	x	x	x	x	x	x	x	x	x	x	x
Oregon	x	x	x	x	x	x	x	x	x	x	x	x	x	x	x	x
Pennsylvania	x	x	x	x	x	x	x	x	x	x	x	x	x	x	x	x
Rhode Island	x	x	x	x	x	x	x	x	x	x	x	x	x	x	x	x
South Carolina	x	x	x	x	x	x	x	x	x	x	x	x	x	x	x	x
South Dakota	x	x	x	x	-0.8	x	x	x	-0.652	x	x	x	0.73	x	x	x
Tennessee	x	x	x	x	x	x	x	x	x	x	x	x	x	x	x	x
Texas	x	x	x	x	x	x	x	x	x	x	x	x	x	x	x	x
Utah	x	x	x	x	x	x	x	x	x	x	x	x	x	x	x	x
Vermont	x	x	x	x	x	x	x	x	0.962	x	x	x	x	x	x	x
Virginia	x	x	x	x	x	x	x	x	x	x	x	x	x	x	x	x
Washington	x	x	x	x	x	x	x	x	x	x	x	x	x	x	x	x
West Virginia	x	x	x	x	x	x	x	x	x	x	0.509	x	x	x	x	x
Wisconsin	x	x	x	x	x	x	x	x	x	x	x	x	x	x	x	x

Table S4. Full state–driver results across all three causal-discovery methods and descriptive Pearson correlation, at the nominal $p < 0.1$ threshold. Note on sign interpretation: PCMCI and Corr (Pearson correlation) values are directional (positive = positive association, negative = inverse association). TE values are non-negative by construction (Section 3.3.2) and reflect the magnitude of information transfer only, not its direction. CCM values (ρ) reflect cross-map prediction skill; while ρ can range from −1 to 1, its sign should not be interpreted as a directional coefficient in the same sense as PCMCI or Corr. Accordingly, apparent differences in sign between TE or CCM and PCMCI/Corr for the same driver–state pair do not represent a contradiction.

	PCPI				Precipitation				Maximum Temperature				Minimum Temperature			
Methods States	PCMCI	TE	CCM	Corr	PCMCI	TE	CCM	Corr	PCMCI	TE	CCM	Corr	PCMCI	TE	CCM	Corr
Alabama	x	0.409	x	0.222	x	x	x	x	0.529	x	x	x	x	x	x	x
Alaska	x	x	0.096	-0.322	x	0.417	x	x	x	x	x	x	x	x	x	x
Arizona	x	x	x	0.296	x	x	x	x	x	x	x	x	x	x	x	x
Arkansas	x	x	x	x	x	0.3	x	0.482	x	x	0.047	x	x	x	x	x
California	x	x	x	x	x	x	x	x	x	x	x	x	x	x	x	x
Colorado	x	x	x	0.28	x	x	x	0.326	0.652	x	x	x	-0.464	x	x	0.245
Connecticut	0.515	x	x	x	x	x	x	x	x	x	x	x	x	0.296	x	x
Delaware	x	x	x	x	x	0.245	x	x	x	x	x	x	x	x	x	x
Florida	-0.549	x	x	x	x	0.272	x	x	x	x	x	x	x	x	x	x
Georgia	x	0.187	-0.061	0.43	x	x	x	x	x	x	x	x	x	x	x	x
Hawaii	x	x	x	x	0.572	x	x	x	x	x	x	x	0.583	0.323	x	-0.326
Idaho	x	x	x	x	x	x	x	x	x	x	x	-0.258	x	0.257	x	x
Illinois	x	x	x	0.262	x	x	x	x	0.875	x	x	x	x	x	x	0.258
Indiana	x	x	x	x	x	x	x	x	x	x	x	0.412	-0.666	x	x	x
Iowa	-0.705	x	x	x	0.627	x	x	x	x	x	x	-0.234	-0.681	x	0.102	x
Kansas	0.527	0.289	x	x	0.606	0.293	x	x	x	0.376	x	x	0.459	0.406	x	x
Kentucky	x	x	x	-0.294	x	x	x	-0.38	x	x	x	x	-0.484	x	x	x
Louisiana	x	0.328	x	x	x	0.241	x	x	0.646	x	x	x	x	x	x	-0.247
Maine	x	x	x	x	x	x	x	x	x	x	x	x	0.633	x	x	x
Maryland	x	x	x	x	x	x	x	x	x	x	x	x	-0.674	x	x	x
Massachusetts	x	x	x	x	x	0.344	x	x	x	x	x	x	x	x	x	x
Michigan	x	x	x	x	x	x	x	x	x	x	x	x	x	0.265	x	x
Minnesota	x	x	x	-0.319	x	0.321	x	0.249	x	0.301	x	x	x	x	x	x
Mississippi	x	x	0.011	-0.233	x	x	0.168	x	0.484	x	x	x	x	x	x	0.23
Missouri	x	x	x	x	x	x	x	x	x	x	x	x	x	x	x	x
Montana	0.543	x	x	x	x	x	x	-0.249	x	x	x	x	-0.545	0.291	x	x
Nebraska	x	x	x	x	x	0.212	x	x	-0.593	x	x	0.248	-0.647	0.181	x	x
Nevada	x	x	0.218	x	x	x	x	x	x	x	x	x	x	x	x	x
New Hampshire	-0.513	x	x	x	x	x	x	x	-0.463	x	x	x	0.51	x	x	x
New Jersey	x	x	0.109	-0.255	x	x	x	-0.303	x	x	-0.031	x	x	x	x	x
New Mexico	x	x	x	x	x	x	x	-0.248	x	x	x	x	0.591	0.186	x	0.239
New York	0.593	x	0.368	-0.257	x	0.248	x	x	x	x	x	x	x	x	x	x
North Carolina	x	x	x	x	x	0.204	x	-0.346	x	x	x	0.244	x	x	x	x
North Dakota	x	x	x	x	x	x	x	x	x	x	x	x	x	x	x	x
Ohio	x	0.365	-0.012	x	x	x	x	x	0.627	x	x	x	x	x	x	x
Oklahoma	0.411	0.31	x	x	x	x	x	-0.36	x	x	x	x	-0.388	x	x	-0.281
Oregon	x	x	0.374	-0.382	x	x	x	x	x	x	x	-0.275	x	x	0.158	-0.353
Pennsylvania	x	x	x	x	x	x	x	x	x	x	x	x	x	x	x	x
Rhode Island	x	x	0.255	x	x	x	x	x	x	x	0.148	x	x	x	x	x
South Carolina	x	x	x	x	x	x	x	x	x	x	x	x	x	x	x	x
South Dakota	x	x	x	x	-0.8	x	x	x	-0.652	x	x	x	0.73	x	x	x
Tennessee	x	x	x	x	x	x	x	x	-0.515	x	x	x	-0.386	x	x	x
Texas	x	x	x	x	x	x	x	x	x	x	x	x	x	x	x	x
Utah	x	x	x	x	x	0.224	x	-0.339	x	0.237	x	0.293	-0.717	x	x	x
Vermont	0.718	x	x	x	x	x	x	x	0.962	x	x	x	x	x	x	x
Virginia	x	x	x	x	x	x	x	x	x	x	x	x	x	x	x	x
Washington	x	0.321	x	x	x	0.313	x	x	x	x	x	x	x	x	x	x
West Virginia	x	0.379	x	0.333	x	0.336	x	x	0.404	0.379	0.509	0.363	x	0.377	x	0.229
Wisconsin	x	x	0.212	-0.243	x	0.294	x	0.326	x	x	x	-0.238	x	x	x	x

Table S5. Full state–driver results across all three causal-discovery methods and descriptive Pearson correlation, restricted to associations surviving FDR correction at $p < 0.1$. Note on sign interpretation: PCMCI and Corr (Pearson correlation) values are directional (positive = positive association, negative = inverse association). TE values are non-negative by construction (Section 3.3.2) and reflect the magnitude of information transfer only, not its direction. CCM values (ρ) reflect cross-map prediction skill; while ρ can range from −1 to 1, its sign should not be interpreted as a directional coefficient in the same sense as PCMCI or Corr. Accordingly, apparent differences in sign between TE or CCM and PCMCI/Corr for the same driver–state pair do not represent a contradiction.

	PCPI				Precipitation				Maximum Temperature				Minimum Temperature			
Methods States	PCMCI	TE	CCM	Corr	PCMCI	TE	CCM	Corr	PCMCI	TE	CCM	Corr	PCMCI	TE	CCM	Corr
Alabama	x	x	x	x	x	x	x	x	x	x	x	x	x	x	x	x
Alaska	x	x	x	x	x	x	x	x	x	x	x	x	x	x	x	x
Arizona	x	x	x	x	x	x	x	x	x	x	x	x	x	x	x	x
Arkansas	x	x	x	x	x	x	x	0.482	x	x	x	x	x	x	x	x
California	x	x	x	x	x	x	x	x	x	x	x	x	x	x	x	x
Colorado	x	x	x	x	x	x	x	x	0.652	x	x	x	x	x	x	x
Connecticut	x	x	x	x	x	x	x	x	x	x	x	x	x	x	x	x
Delaware	x	x	x	x	x	x	x	x	x	x	x	x	x	x	x	x
Florida	x	x	x	x	x	x	x	x	x	x	x	x	x	x	x	x
Georgia	x	x	x	0.43	x	x	x	x	x	x	x	x	x	x	x	x
Hawaii	x	x	x	x	x	x	x	x	x	x	x	x	x	x	x	x
Idaho	x	x	x	x	x	x	x	x	x	x	x	x	x	x	x	x
Illinois	x	x	x	x	x	x	x	x	0.875	x	x	x	x	x	x	x
Indiana	x	x	x	x	x	x	x	x	x	x	x	x	x	x	x	x
Iowa	-0.705	x	x	x	0.627	x	x	x	x	x	x	x	-0.681	x	x	x
Kansas	x	x	x	x	0.606	x	x	x	x	x	x	x	x	x	x	x
Kentucky	x	x	x	x	x	x	x	x	x	x	x	x	x	x	x	x
Louisiana	x	x	x	x	x	x	x	x	x	x	x	x	x	x	x	x
Maine	x	x	x	x	x	x	x	x	x	x	x	x	x	x	x	x
Maryland	x	x	x	x	x	x	x	x	x	x	x	x	x	x	x	x
Massachusetts	x	x	x	x	x	x	x	x	x	x	x	x	x	x	x	x
Michigan	x	x	x	x	x	x	x	x	x	x	x	x	x	x	x	x
Minnesota	x	x	x	x	x	x	x	x	x	x	x	x	x	x	x	x
Mississippi	x	x	x	x	x	x	x	x	x	x	x	x	x	x	x	x
Missouri	x	x	x	x	x	x	x	x	x	x	x	x	x	x	x	x
Montana	x	x	x	x	x	x	x	x	x	x	x	x	x	x	x	x
Nebraska	x	x	x	x	x	x	x	x	-0.593	x	x	x	-0.647	x	x	x
Nevada	x	x	x	x	x	x	x	x	x	x	x	x	x	x	x	x
New Hampshire	x	x	x	x	x	x	x	x	x	x	x	x	x	x	x	x
New Jersey	x	x	x	x	x	x	x	x	x	x	x	x	x	x	x	x
New Mexico	x	x	x	x	x	x	x	x	x	x	x	x	x	x	x	x
New York	x	x	x	x	x	x	x	x	x	x	x	x	x	x	x	x
North Carolina	x	x	x	x	x	x	x	x	x	x	x	x	x	x	x	x
North Dakota	x	x	x	x	x	x	x	x	x	x	x	x	x	x	x	x
Ohio	x	x	x	x	x	x	x	x	x	x	x	x	x	x	x	x
Oklahoma	x	x	x	x	x	x	x	x	x	x	x	x	x	x	x	x
Oregon	x	x	x	x	x	x	x	x	x	x	x	x	x	x	x	x
Pennsylvania	x	x	x	x	x	x	x	x	x	x	x	x	x	x	x	x
Rhode Island	x	x	x	x	x	x	x	x	x	x	x	x	x	x	x	x
South Carolina	x	x	x	x	x	x	x	x	x	x	x	x	x	x	x	x
South Dakota	x	x	x	x	-0.8	x	x	x	-0.652	x	x	x	0.73	x	x	x
Tennessee	x	x	x	x	x	x	x	x	x	x	x	x	x	x	x	x
Texas	x	x	x	x	x	x	x	x	x	x	x	x	x	x	x	x
Utah	x	x	x	x	x	x	x	x	x	x	x	x	x	x	x	x
Vermont	x	x	x	x	x	x	x	x	0.962	x	x	x	x	x	x	x
Virginia	x	x	x	x	x	x	x	x	x	x	x	x	x	x	x	x
Washington	x	x	x	x	x	x	x	x	x	x	x	x	x	x	x	x
West Virginia	x	x	x	x	x	x	x	x	x	x	0.509	x	x	x	x	x
Wisconsin	x	x	x	x	x	x	x	x	x	x	x	x	x	x	x	x